

University of Louisville

ThinkIR: The University of Louisville's Institutional Repository

Electronic Theses and Dissertations

8-2022

Experimental evaluation of heat leak from anti-sweat components into fresh food and freezer compartments of a household refrigerator.

Delva Felissaint
University of Louisville

Follow this and additional works at: <https://ir.library.louisville.edu/etd>



Part of the [Heat Transfer, Combustion Commons](#), and the [Other Mechanical Engineering Commons](#)

Recommended Citation

Felissaint, Delva, "Experimental evaluation of heat leak from anti-sweat components into fresh food and freezer compartments of a household refrigerator." (2022). *Electronic Theses and Dissertations*. Paper 3971.

<https://doi.org/10.18297/etd/3971>

This Master's Thesis is brought to you for free and open access by ThinkIR: The University of Louisville's Institutional Repository. It has been accepted for inclusion in Electronic Theses and Dissertations by an authorized administrator of ThinkIR: The University of Louisville's Institutional Repository. This title appears here courtesy of the author, who has retained all other copyrights. For more information, please contact thinkir@louisville.edu.

EXPERIMENTAL EVALUATION OF HEAT LEAK FROM ANTI-SWEAT
COMPONENTS INTO FRESH FOOD AND FREEZER COMPARTMENTS OF A
HOUSEHOLD REFRIGERATOR

By

Delva Felissaint

B.S., Florida International University, 2018

A Thesis

Submitted to the Faculty of the

University of Louisville

J.B. Speed School of Engineering

In Partial Fulfillment of the Requirements

for the Degree of

Master of Science

in Mechanical Engineering

Department of Mechanical Engineering

University of Louisville

Louisville, KY

August 2022

EXPERIMENTAL EVALUATION OF HEAT LEAK FROM ANTI-SWEAT
COMPONENTS INTO FRESH FOOD AND FREEZER COMPARTMENTS OF
HOUSEHOLD REFRIGERATOR

By

Delva Felissaint

B.S., Florida International University, 2018

A Thesis Approved On

August 8th, 2022

by the following Thesis Committee:

Dr. Ellen Brehob, Thesis Co-Advisor

Dr. Andrea Kelecy, Thesis Co-Advisor

Dr. R. Eric Berson, Committee Member

DEDICATION

This thesis is dedicated to my parents, Delices and Beatrice Felissaint, who have shown me through their tireless work ethic that all things are achievable with enough perseverance, and to the love of my life, Ada Mileny Salgado, who has given me the strength and motivation to pursue my dreams and find the light in the darkest of times.

ACKNOWLEDGMENT

I would like to thank my advisors, Dr. Brehob and Dr. Kelecy for their continual support and advice provided to me throughout this study. Additionally, I would like to thank my mentors at GE Appliances, Marty Zentner and Carlos Herrera, for providing me with the resources needed for the experiment as well as being exemplary role models for a novice engineer.

ABSTRACT

EXPERIMENTAL EVALUATION OF HEAT LEAK FROM ANTI-SWEAT COMPONENTS INTO FRESH FOOD AND FREEZER COMPARTMENTS OF HOUSEHOLD REFRIGERATOR

Delva Felissaint

August 8th, 2022

Condensation beads forming on outside surfaces around a refrigerator is an undesirable byproduct driven by the cold temperature exhibited throughout the unit. To combat this issue, anti-sweat components usually in the form of electrical heaters or tubes carrying hot refrigerant, bring heat to the cold surfaces to ensure their temperatures do not drop below the dew point. Some heat produced by the anti-sweat components may transfer to the interior refrigerated compartment. The purpose of this study is to quantify how much heat from the anti-sweat components are entering the fresh food and freezer compartments and what impact that has on the energy usage and thermal performance of the unit.

A dual evaporator, single damper refrigerator-freezer was the test model in this experiment and a forward heat leak calorimeter provided the capability of determining the amount of heat entering the cabinet. It was found from a forward

heat leak calorimeter system, that 74% of the 2.4 W load from the hot liquid loop, 71% of the 10.9 W load from the articulating mullion heater, 32% of the 5 W load from the icebox gasket heater and 52% of the 10.5 W load from Door-in-Door heater entered the cabinet.

An AMESIM simulation model was used to evaluate the additional compressor power consumed by the introduction of the additional heat into the cabinet. The impact of the hot liquid loop and heaters (assuming a 100% operation) is an additional 17.6 W or 66.5 kWhr/year compressor power required to remove the heat leaking into the cabinet. This is not a negligible impact as the total energy reported by the DOE in 2021 was 757 kWhr/year. Additional work may need to be done to optimize usage of these components and reduce the energy impact.

TABLE OF CONTENTS

DEDICATION	iii
ACKNOWLEDGMENT	iv
ABSTRACT	v
LIST OF TABLES	x
LIST OF FIGURES	xii
1 INTRODUCTION	1
1.1 Previous Studies Investigating the Effect of Heat Leak on Performance of Refrigerators	4
1.2 Previous Studies on Vapor Mass Quality of Refrigerant.....	7
1.3 Previous Studies of Refrigeration Modeling.....	12
2 EXPERIMENTAL PROCEDURES	18
2.1 Experimental Setup for Quantifying Heat from Hot Liquid Loop	20
2.2 Forward Heat Leak Calorimeter System.....	27
2.3 Household Refrigerator-Freezer used in Forward Heat Leak Testing ...	29

2.4	Proportional Integral (PI) Control of Different Components & LabView Interface	33
2.5	Modeling Heat Loads of Anti-Sweat Components in Forward Heat Leak (FWHL) System.....	38
3	MODELING PERFORMANCE OF REFRIGERATOR WITH AMESIM.....	44
3.1	Background on AMESIM Software	44
3.2	Construction of Household Refrigerator/Freezer Model in AMESIM	46
3.3	Creation of Supercomponents used in AMESIM Model.....	51
3.3.1	Modeling of Compressor as Supercomponent in AMESIM.....	51
3.3.2	Modeling Heat Exchangers as Supercomponents in AMESIM	55
3.3.3	Modeling Fans as Supercomponents in AMESIM.....	57
3.3.4	Creation of Refrigerator/Freezer Cabinet and the Control Algorithm	59
4	RESULTS	63
4.1	Heat Quantification Test Results	63
4.2	Forward Heat Leak Test Results	66
4.2.1	Electrical Anti-Sweat Heaters Test Data	66
4.2.2	Hot Liquid Loop Data	75
4.2.3	Summary of Forward Heat Leak Test Results	77
4.2.4	Repeatability Testing for Forward Heat Leak Experiment.....	78

4.3	AMESIM Model Test Results.....	79
4.4	Uncertainty Calculations with Test Results.....	82
5	CONCLUSIONS.....	85
5.1	Important Results	85
5.2	Future Work & Conclusion.....	87
	REFERENCES.....	90
	CURRICULUM VITA	92

LIST OF TABLES

Table 1-1 Annual Energy Usage of a Refrigerator at the national average of \$0.12/kWH.....	2
Table 1-2 AMESIM study performed on Top Mount Refrigerator showing correlation between compartment temperatures and compressor runtime.....	16
Table 2-1 Variables and their measurements methods used in Heat Quantification of Hot Liquid Loop Experiment	25
Table 2-2 Summary of PI controlled variables and their respective process variables	38
Table 2-3 Rated heater wattages of the electrical heater anti-sweat components	39
Table 2-4 Variables and measurement methods used to control hot water system heat load.....	43
Table 3-1 Internal Volumes of refrigerated compartments of experimental study unit.....	47
Table 3-2 Materials used in AMESIM model and their thermal conductivities	50
Table 4-1 Summary of Forward Heat Leak Test Results for each Anti-Sweat Component; *Scaled up heat load to model hot liquid loop in FWHL.	78
Table 4-2 Repeated test results of the Forward Heat Leak Experiment	79

Table 4-3 AMESim Model Results given additional heat leak inputs from anti-sweat components.....	81
Table 4-4 Uncertainty Calculation for the heat leak results in Hot Water System Liquid Loop	83
Table 4-5 Uncertainty Calculation of the heat leak results for the Forward Heat Leak System.....	84

LIST OF FIGURES

Figure 1-1 Schematic showing anti-sweat component locations in household refrigerator-freezer unit. (1) Hot Liquid Loop, (2) Articulating Mullion Heater, (3&4) Icebox Gasket Heater and Ice Recess Heater, (5) Door-In-Door Heater	4
Figure 1-2 Freezer cabinet temperature during the defrost cycle (Zhao et al., 2007)	5
Figure 1-3 Schematic of gas-matrix system for sensible refrigeration storage	6
Figure 1-4 Experimental apparatus of standard automotive air conditioning hermetic system with instrumentation (Wang et al., 2005)	11
Figure 1-5 The calculated COP values of the air conditioning system for 1000 W/m ² solar load	14
Figure 1-6 Compressor runtime and Unit Power comparison between Integrated Product and AMESIM model	15
Figure 2-1 Sealed System Schematic of Household Refrigerator Used for Study	18
Figure 2-2 Pressure-Enthalpy Diagram Illustrating Vapor Quality Range of Hot Liquid Loop Refrigerant	19
Figure 2-3 Instrumentation used for Heat Load Quantification of HLL showing RTD, differential pressure sensor at outlet of HLL, and absolute pressure sensor at compressor suction	22

Figure 2-4 Instrumentation used for Heat Load Quantification of Hot Liquid Loop showing RTD and absolute pressure sensor at inlet of HLL.....	22
Figure 2-5 Agilent Data Card for RTD and Pressure Readings	24
Figure 2-6 Schematic showing measurement locations of the sensors	26
Figure 2-7 Back view showing instrumentation used on the Heat Quantification Unit.....	26
Figure 2-8 Schematic of instrumented forward heat leak calorimeter (Berghuis, 2020)	28
Figure 2-9 Forward Heat Leak System Connected to Household Refrigerator used for this study	30
Figure 2-10 Copper Tubes from Forward Leak Calorimeter System fed from side of the case into the FF compartment.....	30
Figure 2-11 Insulated copper FF evap suction line in test unit used in Forward Heat Leak calorimeter system	32
Figure 2-12 Diagram showing Thermostatic Expansion Valve construction in FWHL system.....	33
Figure 2-13 LabView Interface of Control and Measured Parameters for Forward Heat Leak System	35
Figure 2-14 Temperature illustrating the PI tuning process for the TXV in the freezer compartment	37
Figure 2-15 Schematic of hot water system used in forward heat leak.....	41
Figure 2-16 Photo of hot water system used in forward heat leak.....	41

Figure 2-17 Photo of hot water system entering in forward heat leak system test unit.....	42
Figure 3-1 Schematic showing simple mass-spring damper system modeled using bond graph theory	45
Figure 3-2 Example of AMESIM being used to create thermal model of a refrigerator wall.....	46
Figure 3-3 System Level View of test unit Refrigerator Unit Modeled in AMESIM	48
Figure 3-4 Compressor supercomponent modeled in AMESIM	52
Figure 3-5 Compressor angular velocity, cooling capacity, and compressor power interpolator modeled in AMESIM.....	54
Figure 3-6 Fresh Food Evaporator	55
Figure 3-7 AMESIM Model of Fresh Food Evaporator supercomponent	56
Figure 3-8 FF Fan supercomponent modeled in AMESIM	58
Figure 3-9 Airflow Test setup for convertible drawer flow measurement	59
Figure 3-10 CREO Model of French Door Test Product	60
Figure 3-11 Fresh Food Cabinet supercomponent.....	61
Figure 4-1 Heat load and subcooling at the inlet of hot liquid loop plotted over compressor on cycle.....	64
Figure 4-2 Compartment temperature stability in Heat Quantification Unit during compressor on cycle.....	65
Figure 4-3 Baseline Heat Leak in the Fresh Food Compartment.....	67
Figure 4-4 Baseline Heat Leak in the Freezer Compartment	68

Figure 4-5 Heat Leak with Mullion Heater on in the FF Compartment.....	69
Figure 4-6 Heat Leak with Mullion Heater on in the FZ Compartment.....	69
Figure 4-7 Anti-Sweat Heater inside Door in Door Liner.....	70
Figure 4-8 Heat Leak with Door-In-Door Heater on in the FF Compartment	71
Figure 4-9 Heat Leak with Door-In-Door Heater on in the FZ Compartment	71
Figure 4-10 Heat Leak with Icebox Gasket Heater on in the FF Compartment ..	72
Figure 4-11 Heat Leak with Icebox Gasket Heater on in the FZ Compartment ..	73
Figure 4-12 Heat Leak with Ice Dispenser Heater on in the FF Compartment ...	74
Figure 4-13 Heat Leak with Ice Dispenser Heater on in the FZ Compartment ...	74
Figure 4-14 Heat Leak with Hot Liquid Loop on in the Fresh Food Compartment	76
Figure 4-15 Heat Leak into the FZ Compartment with Hot Liquid Loop Activated	77
Figure 4-16 Comparison between AMESIM model and test data from a real unit	80

1 INTRODUCTION

A vast majority of household refrigerator-freezers utilize a hermetic refrigerant system to remove heat from cooled compartments and maintain desirable temperatures for food and drink storage. Condensation occurs as moisture laden ambient air comes into contact with a surface that is cold enough to bring the water vapor in the air below its dew point temperature. Based on GE Appliances consumer data, the average consumer's home is anywhere between 20°C (68°F) and 24.4°C (76°F) with a relative humidity ranging between 30-50%. Given the wide range of ambient conditions a unit may be placed in, it is likely that surface condensation will occur under normal conditions as some compartments are required to go to sub-zero temperatures. Areas around the refrigerator-freezer may get below dew point temperatures and cause pockets of sweat (condensation beads) on the outside surface that is visible to the consumer. Puddles of water can form because of this, which is unappealing as well as potentially being a slipping hazard to the user.

To combat this issue, anti-sweat components are installed in the refrigerator whose purpose is to bring heat to the problem area and drive the surface temperature above the dew point to prevent sweat from occurring. A portion of the heat will be rejected to the ambient and some portion will move into the refrigerated compartment. This additional heat will affect how the unit

behaves as it seeks to maintain temperatures, driving higher compressor run times and energy usage. As reference, a typical GEA French door 28 ft³ household refrigerator consumes around 750 kWh/year of electricity (Appliances and Refrigerator, 2022) which would equate to \$126 in energy costs a year in the state of California. Energy Star, which is a certification that shows a product is well below the energy margin set by the Department of Energy (DOE), is a government-backed symbol for energy efficiency and is an increasingly important distinction. With the world advancing towards more energy saving initiatives as well as the DOE constantly decreasing the energy consumption limit for appliances, the utilization of energy efficient operating strategies is extremely important in the design of these appliances. Table 1-1 shows the difference in total annual energy consumption of a refrigerator 35 years apart.

Year	Energy Usage [kWh/year]	Cost to Operate/Year [\$]
1986	1400	168
2021	757	91

Table 1-1 Annual Energy Usage of a Refrigerator at the national average of \$0.12/kWH

The major goals of this study are,

- i) Quantify the total heat loads from each of the anti-sweat components
- ii) Determine the fraction of heat dissipated (heat leak) into the compartment from the anti-sweat components
- iii) Predict the impact to compressor energy usage based on the heat leak values from the anti-sweat components

A GEA French door refrigerator-freezer was the test unit of interest for this study. The anti-sweat components referenced throughout this paper were four different electrical heaters and a “hot liquid loop” (HLL), which is a steel tube carrying hot refrigerant from the condenser outlet to the front face of the freezer. It also passes through the convertible drawer area, which is a compartment that has the capability of converting into either a Fresh Food (FF) or Freezer (FZ) region and the temperature range is 23 °F to 42 °F. The location of the anti-sweat components is shown in Figure 1-1.



Figure 1-1 Schematic showing anti-sweat component locations in household refrigerator-freezer unit. (1) Hot Liquid Loop, (2) Articulating Mullion Heater, (3&4) Icebox Gasket Heater and Ice Recess Heater, (5) Door-In-Door Heater

1.1 Previous Studies Investigating the Effect of Heat Leak on Performance of Refrigerators

A primary goal of this study was to understand the impact of the heat leaked into the compartment(s) from the operation of the anti-sweat components. Having a better understanding of the role heat leak played on refrigerator performance and energy use in different test scenarios helps to design better performing, higher efficiency refrigerators. The following studies looked at the effect of heat leak on the performance of refrigerators.

A study performed by (Zhao et al., 2007) investigated the effect of defrost heat leakage on freezer temperature rise. The experiment was performed on a single evaporator, single air damper, frost-free refrigerator-freezer that was instrumented with seven T-type thermocouples in the evaporator and the freezer compartment area. A tubular metal sheathed heater installed upstream of the evaporator was used to simulate the defrost cycle. The test was conducted in a climate-controlled chamber conforming to ISO 8561 Standard, ambient temperature was at 25 ± 0.5 C and RH at about 60%, unit operated in cyclic nature between cut-in and cut-out temperatures of -18°C and -21 C, respectively. The results of the experiment showed that at its peak stage (period where compartment temperatures were highest), the defrost heater contributed to a 1 C/min rise in freezer temperature.

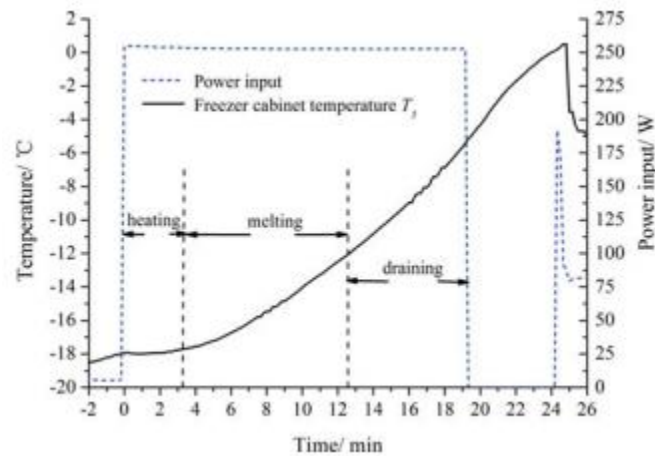


Figure 1-2 Freezer cabinet temperature during the defrost cycle (Zhao et al., 2007)

Sahoo (1987) looked at a typical refrigeration storage unit where the cooling is performed by a cold gas stream that exhausted in the environment and

heat is exchanged with the ambient (shown in Figure 1-3). A numerical analysis utilizing the Second Law of Thermodynamics for a sensible refrigeration energy storage unit showed that heat leak from the environment had a noticeable effect on the entropy production of the system and that the useful work stored in the unit is severely impacted by the amount of heat leak across the system.

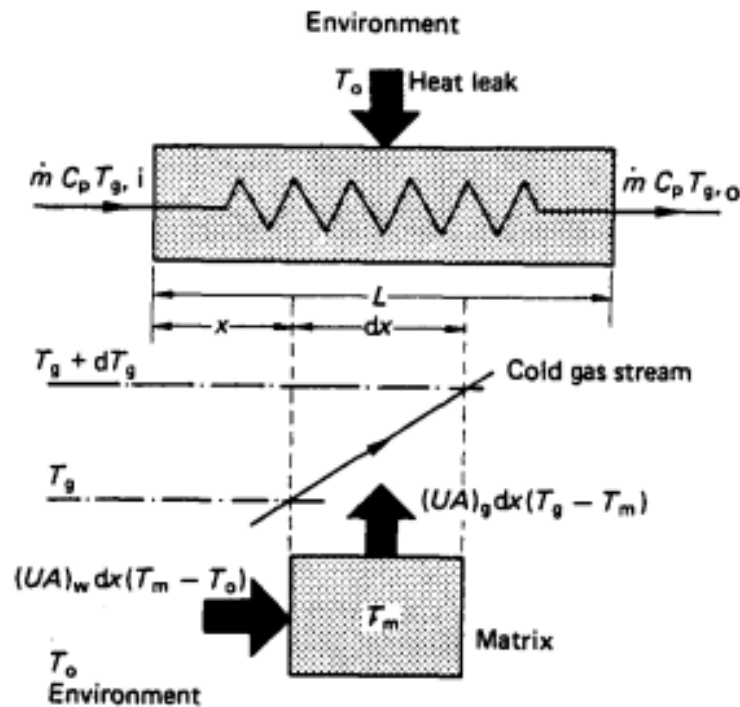


Figure 1-3 Schematic of gas-matrix system for sensible refrigeration storage

Ameel (2009) developed a numerical model to study the performance of a parallel-flow heat exchanger while both fluid streams are being affected by the ambient surroundings. It was found that as the temperature difference between the ambient and the working fluid increased, the effectiveness of the heat exchanger decreased. (Alquaity et al., 2013) similarly explored a numerical model looking at the effects of external heat leak on the performance of a heat

exchanger but considered the effect kinetic energy variation as well. It was found that an increase in heat leak on the cold side of the heat exchanger drastically lowered the effectiveness of the heat exchanger. Results from the articles mentioned in this section illustrate the large impact heat leak can have on refrigerator performance.

1.2 Previous Studies on Vapor Mass Quality of Refrigerant

While most of the anti-sweat components are electrical, the hot liquid loop uses heat from the high temperature refrigerant exiting the condenser. To determine the heat loss rate of the hot liquid loop, the refrigerant state needs to be defined at the inlet and outlet. It is unknown if the refrigerant exiting the condenser is subcooled or two-phase, and further, if the refrigerant is underneath the vapor dome (two-phase), pressure and temperature are not enough to fully define the state and extract an enthalpy value. In case the refrigerant is indeed two-phase at the condenser exit, a method to determine the vapor quality is needed. The following studies explain different methods in which quality was determined in different two-phase systems.

An experimental study (Dalkilic et al. 2011) was performed to determine the condensation heat transfer coefficients of R134A in a vertical smooth tube. In order to effectively model the heat transfer coefficients, the vapor quality of the refrigerant had to be determined. The refrigerant is circulated throughout the system by a gear pump. A double tube heat exchanger supplied heat to the refrigerant before entering the test section in order to maintain consistent

conditions and heat was removed after the test by a tube-in-tube heat exchanger. A total of ten T-type thermocouples were used to measure the refrigerant and tube wall temperatures and the test section was insulated to minimize heat loss. The quality of the refrigerant before entering the test section was calculated using Equation 1.

$$x_{TS,i} = \frac{i_{TS,i} - i_{l@T_{TS,i}}}{i_{fg@T_{TS,i}}} \quad (1)$$

$x_{TS,i}$ is vapor quality and $i_{TS,i}$ is the enthalpy of the inlet test section refrigerant, $i_{l@T_{TS,i}}$ and $i_{fg@T_{TS,i}}$ are the inlet enthalpies of the saturated liquid and of vaporization, respectively. This is the standard equation for vapor quality.

Equation (2) illustrates how the enthalpy of the refrigerant was calculated

$$i_{TS,i} = i_{ph,i} + \frac{\dot{q}_{ph}}{\dot{m}_{ref}} \quad (2)$$

$i_{ph,i}$ is the enthalpy of the liquid refrigerant before entering the preheater, \dot{m}_{ref} is the mass flow rate of the refrigerant and \dot{q}_{ph} (calculated from Equation 3) is the heat transfer rate in the preheater. The assumption is that all the heat from the water in the preheater section is transferred to the refrigerant. Since $i_{ph,i}$ is all liquid, temperature and pressure are enough to determine the enthalpy.

$$\dot{q}_{ph} = \dot{m}_{w,ph} c_{p,w} (T_{w,i} - T_{w,o})_{ph} \quad (3)$$

$\dot{m}_{w,ph}$ is the mass flow rate of the water entering the preheater, $c_{p,w}$ is the specific heat of water and $(T_{w,i} - T_{w,o})_{ph}$ is the temperature difference between the inlet and outlet of the preheater water. The process for calculating the outlet

vapor quality was the same. Uncertainties in this measurement method are attributed to the thermocouple instrumentation uncertainty and the adiabatic heat exchange assumption between the water and refrigerant.

(Li et al., 2017) looked at the difference in performance of a condenser with and without phase separation. The experiment was done on a mobile air conditioning system with two different microchannel condensers; the first baseline run was with a standard condenser and the other test was with a separation condenser. The heating capacity of the condenser was calculated by averaging the heating capacities of the airside and refrigerant-side heat transfer.

$$\dot{q}_{ca} = \dot{m}_{ca}(h_{odn} - h_{cai}) \quad (4)$$

$$\dot{q}_{cr} = \dot{m}_{cr}(h_{cri} - h_{cro}) \quad (5)$$

$$\dot{q}_c = \frac{\dot{q}_{cr} + \dot{q}_{ca}}{2} \quad (6)$$

Shown in Equations 4-6, \dot{q}_{ca} was the air side heat transfer, \dot{q}_{cr} was the refrigerant side heat transfer and \dot{q}_c was the average between the two. The results of the study were compared against a condenser model created by the authors. At the same refrigerant inlet and exit temperature, a maximum of 7.4% increase in terms of the mass flow rate and 5.1% for the heating capacity was found in the separation condenser over the conventional condenser. This study highlighted how large the impact of having two-phase refrigerant as opposed to single phase can have on a heat exchanger system.

Vapor quality and its effects on the performance of an automotive air conditioning system was investigated by (Wang et al., 2005). Figure 1-4 shows a standard automotive air conditioning hermetic system with the instrumentation used for the experiment. The vapor quality for the purpose of this study was defined as the ratio of the gas flow rate to the total mass flow rate. The total mass flow rate included the lubrication oil because it would have been nearly impossible to separate the liquid refrigerant and the oil. A mass flow meter was placed after the condenser to record the total mass flow and a sight glass was placed right after to ensure the flow was fully subcooled. Prior to entering the compressor, the refrigerant entered a separator that separated the liquid and gas components. A vapor mass flow meter was placed in the vapor section so the gas mass flow rate could be recorded, and a sight glass was used to ensure the flow was fully gas. The flows merged back together after being separated and before entering the compressor. With both the gas and total mass flow rate, the vapor quality was defined.

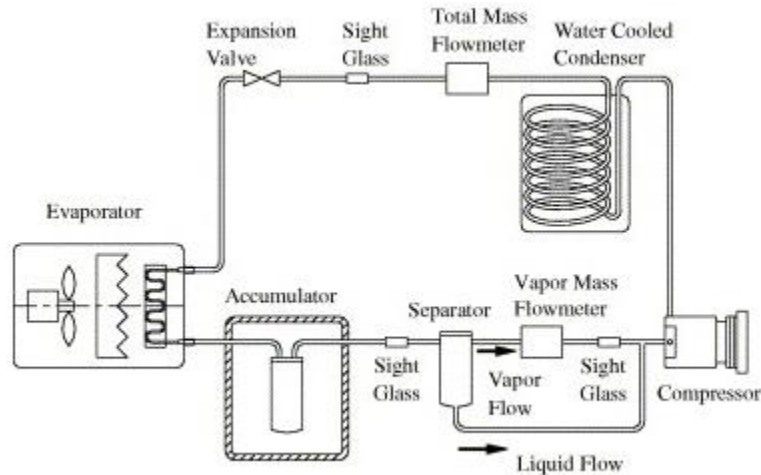


Figure 1-4 Experimental apparatus of standard automotive air conditioning hermetic system with instrumentation (Wang et al., 2005)

From the study it was determined that the vapor quality at the inlet of the compressor is directly related to the coefficient of performance of the cooling system. The author commented that the direct function between the refrigerant quality and its impact on compressor efficiency and system performance will be explored in a future study. A separate study, (Dorfman et al., 2006) referenced multiple methods in which the quality of a refrigerant can be determined, such as the throttling process, mechanical separation, or an electrical calorimeter.

Articles in this section described various methods in which vapor quality was determined, none of which were relatively straightforward as entire systems and controls were implemented in order to obtain accurate measurements. If vapor quality was a necessary parameter that needed to be measured, additional development would be required in order to ensure quality results were achieved.

1.3 Previous Studies of Refrigeration Modeling

The primary objective of this study was to understand what the effect of the heat coming from the anti-sweat components had on the energy use and thermal performance of the refrigerator-freezer unit. Once the heat was quantified from testing, a model of the refrigerator that could determine the difference in energy usage of the compressor given the different heat leaks entering the cabinet had to be created. Numerical models as well as computer simulation models that could potentially achieve this goal were reviewed in this literature survey.

The creation of a classical Carnot refrigeration numerical model that could incorporate all conceivable irreversible processes was completed by (Chen et al., 1997). The paper presented results for six different cases of a refrigerator model, with and without heat leak, no internal irreversibility, with external heat resistance, an infinitely large heat exchanger, and a heat leak only model. The maximum coefficient of performance as well as the corresponding cooling capacity were the main outputs of interest in the model. Additional research in a study by the same author explored the model more in-depth (Chen et al., 1998) and looked at the impact of external heat resistances and heat leak on the performance of refrigerators

(Zhang et al., 2015) did a numerical analysis on a thermosyphon loop to generate a general model that could incorporate a partially liquid as well as a fully liquid downcomer. The results from the experiment were first obtained mathematically using heat transfer correlations for single phase convection,

boiling and condensation, and then experimentally in a psychrometric calorimeter test chamber. Results showed that the heat transfer rate initially increased with additional refrigerant charge and then after a while began to decrease with additional refrigerant charge.

Some of the key observations made with the numerical models presented in this survey were that the solutions had to be general by design, limited by steady-state application and would have no practical way to validate results presented from the analytical solutions. Due to the unique cabinet construction and various cooling components used in the refrigerator-freezer, it was clear a more specific simulation solution would be needed. A key goal of this study was to understand impact to the compressor energy given various heat leak values, therefore a more practical simulation tool that was capable of transient solutions and numerous inputs was explored.

A study performed by (Sevilgen et al., 2020) looked at a one-dimensional analysis of a cool down simulation in a vehicle HVAC system using R-134a and R-1234yf as refrigerants. AMESIM was the simulation tool used for the analysis and it was able to evaluate the thermal performance of the two refrigerants in terms of energy consumption. The cool down scenario in HVAC testing refers to the situation where the cabin interior of a car (SUV in this study) is soaked in the sun and is required to pull down to a certain temperature under a certain amount of time once the HVAC system is turned on. The study modeled the scenario using two different refrigerants and compared the results of the two refrigerants. The model yielded a specific solution to the vehicle being tested as surface area,

inclination angle of the surfaces, thickness of the cabin exterior walls, material, thermal and optical properties of vehicle components, solar radiation, ambient temperature and humidity, the color of the vehicle (which affects the emissivity) and vehicle speed were all included in the simulation.

The AMESIM simulation model for the cool down scenario was able to report values for the average cabin temperature across different solar loads and driving conditions, as well as the coefficient of performance (COP shown in Equation 7) for a solar load of $1000 \frac{W}{m^2}$ over a period of 1200 seconds. The results from the study are shown in Figure 1-5.

$$COP = \frac{\text{Heat absorbed at the Evaporator}}{\text{Compressor Power}} \quad (7)$$

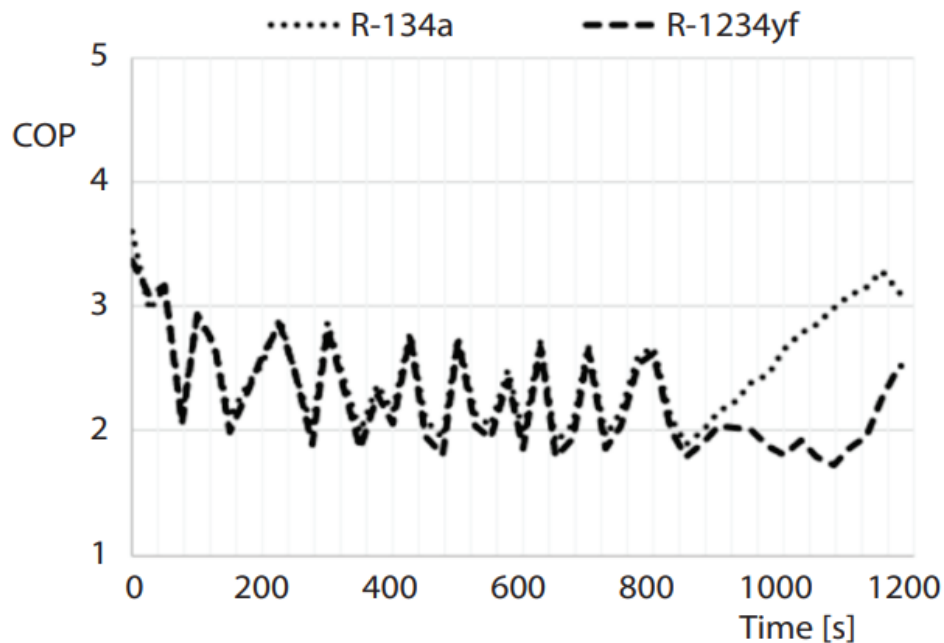


Figure 1-5 The calculated COP values of the air conditioning system for 1000 W/m^2 solar load

Due to its versatility, AMESIM is used across a multitude of different industries such as but not limited to automotive, marine, and aerospace/defense. The software has the capability for either steady-state or transient solutions and since the study was concerned with the energy usage of the compressor, the solution needed to be transient. There have previously been studies conducted at GE Appliances by Herrera (2018,2019) that focused on modeling refrigerator-freezer models and component optimization based on energy usage. Selected results from previous studies are shown in Figure 1-6 and Table 1-2.

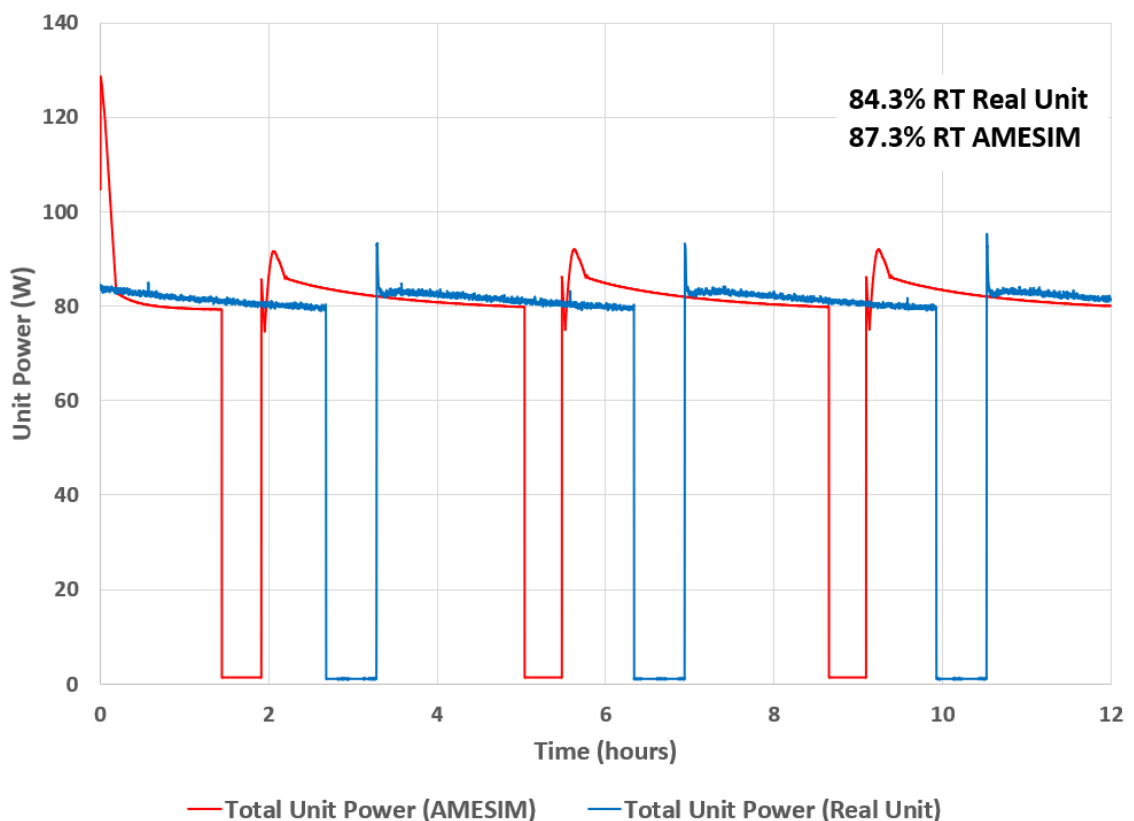


Figure 1-6 Compressor runtime and Unit Power comparison between Integrated Product and AMESIM model

	FF avg temperature [°F]	FZ avg temperature [°F]	Compressor Runtime
Top Mount Refrigerator (actual)	41.58	5.11	46.4%
AMESIM (simulation)	41.53	6.77	45.8%
Difference	0.05	1.66	0.6%

Table 1-2 AMESIM study performed on Top Mount Refrigerator showing correlation between compartment temperatures and compressor runtime

Figure 1-6 shows results from a study performed on an Integrated Refrigerator model. An AMESIM model was constructed to predict the impact to compressor run time with varying condenser airflow. The graph displays the initial comparison of compressor power versus time and the discontinuous points where the compressor power is nearly 0 indicates to the off cycles of the compressor. The initial version of the model was compared against a physical unit and found the simulation and real unit were within 3% RT of one another. The compressor run time percent is shown in Equation 8 and taken as

$$Compressor\ RT\% = \frac{Compressor\ On\ Time}{Total\ Compressor\ Time} \quad (8)$$

Table 1-2 was a study conducted on a top mount refrigerator with compressor run time % and average compartment temperature reported as outputs. The AMESIM model was constructed as a predictive tool using the geometry and cooling component data as the inputs. The results from the AMESIM model provided design guidance for the product and was then compared against a real unit.

Observing the results for the test studies, there was a high correlation between data from the simulation model and physical model. The accuracy of these studies provided enough confidence to utilize the software in this study. Given the ability for transient solutions and the capability of accepting a multitude of input parameters to can accurately model real-life applications, AMESIM appeared to be a valid tool for the purposes of this study.

2 EXPERIMENTAL PROCEDURES

There are multiple anti-sweat components in the household refrigerator-freezer unit that are used to avert condensation formation. The methods used to quantify the heat from these components that leaks into the refrigerated compartments is described in the following paragraphs. The diagram in Figure 2-1 shows the sealed system configuration of the dual evaporator single damper experimental unit that was used in this study. The unit was a dual-evaporator (located in the FF and FZ compartments), has a water/ice dispenser on the left-hand door as well as a convertible drawer that has a user setpoint range of 23°F - 42°F that was temperature controlled by a damper connected to the FZ.

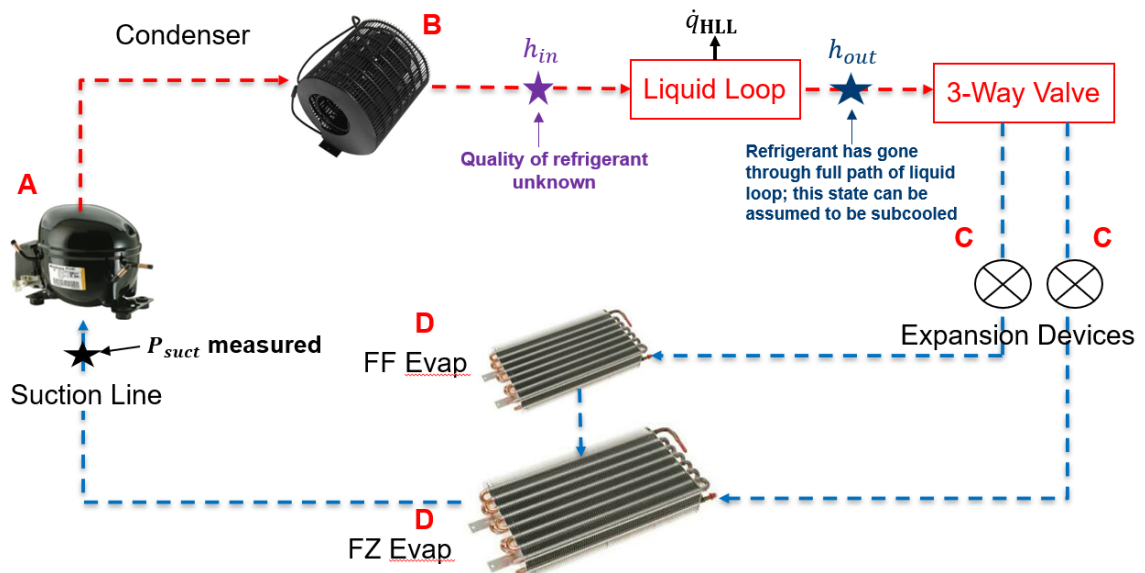


Figure 2-1 Sealed System Schematic of Household Refrigerator Used for Study

An ideal vapor-compression refrigeration cycle is shown in Figure 2-2.

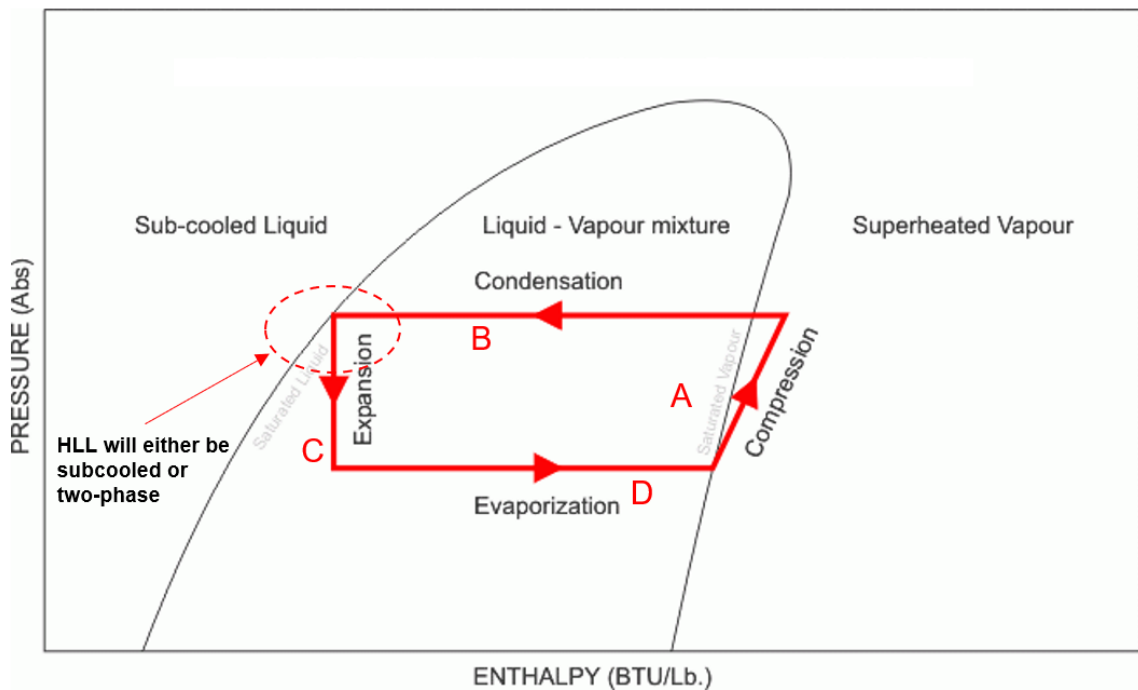


Figure 2-2 Pressure-Enthalpy Diagram Illustrating Vapor Quality Range of Hot Liquid Loop Refrigerant

Low pressure R600a (Isobutane) vapor refrigerant passes through the compressor, where a reciprocating piston compresses the refrigerant and turns it into a high-pressure vapor. It then travels to the condenser where there is heat exchange with the ambient and the vapor condenses into a high temperature high pressure liquid. After that, the refrigerant enters the 3-way valve which directs the flow to either the FF or FZ evaporator by means of a capillary tube. The capillary tubes are small diameter copper tubes that provide the most restriction in the system and act as flow metering components. Immediately afterwards, it goes through the expansion device which is an isenthalpic process where the refrigerant enters a larger diameter portion and converts into a low-

pressure low temperature refrigerant. The cold refrigerant travels through the fresh food and freezer heat exchangers and is responsible for removing heat from the respective compartments.

Referencing Figure 2-1, the hot liquid refrigerant that exits the condenser between stage B and C enters what is referred to as the hot liquid loop (HLL). The HLL is a 0.31-inch diameter steel tube that circulates the refrigerant around the freezer and convertible drawer liner face to provide additional heat to the area and prevent the formation of condensation. The location of the HLL path is shown in Figure 1.1

2.1 Experimental Setup for Quantifying Heat from Hot Liquid Loop

The equation used to calculate the total rate of heat dissipated by the hot liquid loop is shown in Equation 9

$$\dot{q}_{HLL} = \dot{m} \cdot (h_{in} - h_{out}) \quad (9)$$

where \dot{m} is the mass flow rate of the refrigerant, h_{in} is the enthalpy at the inlet of the liquid loop (outlet of the condenser) and h_{out} is the outlet enthalpy of the liquid loop (before the 3-way valve).

To quantify the total heat loss from the hot liquid loop (HLL), it is necessary to define the states at the inlet and outlet locations. The outlet of the HLL will be subcooled as there is substantial enough heat loss as the loop travels across the FZ liner to bring the refrigerant outside the dome. However, at the HLL inlet directly after the condenser, the refrigerant will either be fully subcooled

or a two-phase liquid. If the refrigerant is outside the dome, temperature and pressure are sufficient in defining the enthalpy values. On the other hand, if the refrigerant is under the dome, vapor quality is an additional parameter that would need to be known to determine the enthalpy at that position. Some methods were discussed in the literature section that described obtaining vapor quality from means such as a discharging calorimeter or calculation of vapor and liquid mass for example.

Resistance Temperature Detectors (RTDs) as well as pressure sensors were used at the inlet and outlet positions of the hot liquid loop to determine the temperature and pressure at the given locations to define enthalpy at the inlet and outlet of the HLL. An absolute pressure sensor (0-100 psia) was used at the suction of the compressor as well as the inlet to the hot liquid loop (0-200 psia). A differential pressure sensor was used between the outlet and inlet of the hot liquid loop (0-50psia) to determine the outlet pressure. Pictures of the test unit installed with the instrumentation are shown in Figures 2-3, 2-4 and 2-7. Locations of the sensors relative to the construction of the hermetic system are found on Figure 2-6.

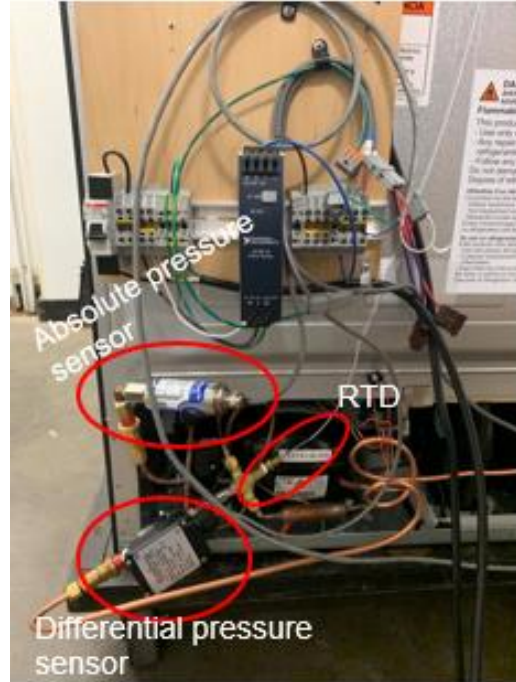


Figure 2-3 Instrumentation used for Heat Load Quantification of HLL showing RTD, differential pressure sensor at outlet of HLL, and absolute pressure sensor at compressor suction

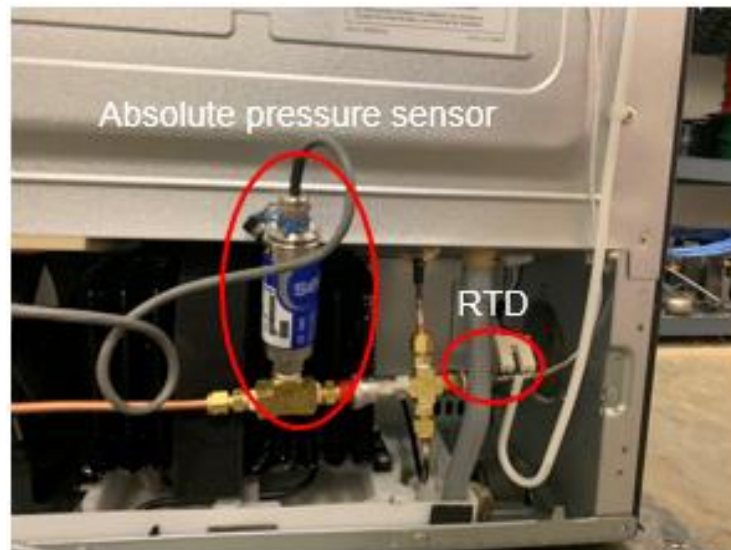


Figure 2-4 Instrumentation used for Heat Load Quantification of Hot Liquid Loop showing RTD and absolute pressure sensor at inlet of HLL

As shown in Equation 9, the mass flow needed to be determined to define the total heat loss from the HLL. The Air-Conditioning, Heating, and Refrigeration Institute STANDARD 540-215 references the method in which manufacturers are required to calculate the compressor power input, mass flow rate and refrigerating capacity. While the standard uses suction and discharge dew point temperature in the correlation, for the purposes of this experiment the suction and discharge pressures were chosen as the input variables instead as the measurement uncertainty with the pressure transducers were considerably less when compared to RTD measurements. A least squares regression polynomial equation was generated using experimental data from compressor calorimeter testing. A total of 11 test points were obtained at a specified compressor frequency of 85 Hz. The suction temperature was fixed at 90 degrees F while the suction and discharge pressures were varied at the different test points. A polynomial was created (Eqn. 10) using the suction and discharge pressures as to determine the mass flow rate.

$$\dot{m} = C_1 + C_2 * P_s + C_3 * P_d + C_4 * P_s^2 + C_5 * (P_s * P_d) + C_6 * P_d^2 + C_7 * P_s^3 + C_8 * (P_d * P_s^2) + C_9 * (P_d * P_s^2) + C_{10} * P_d^3 \quad (10)$$

C_1 through C_{10} are the regression coefficients calculated from the calorimeter data, P_s is the suction pressure and P_d is the discharge pressure.

NPT and brass cross fittings were used throughout the unit and Teflon tape was wrapped around the threading of the NPT fittings to ensure the seal of system. To capture the data, an Agilent data card was used to read the data from the

sensors. The output signal from the pressure sensors was a 4-20 mA signal and was converted into a voltage signal using a 560-ohm resistor. Figure 2-5 shows the Keysight 34970A data card used for the RTD and pressure readings.

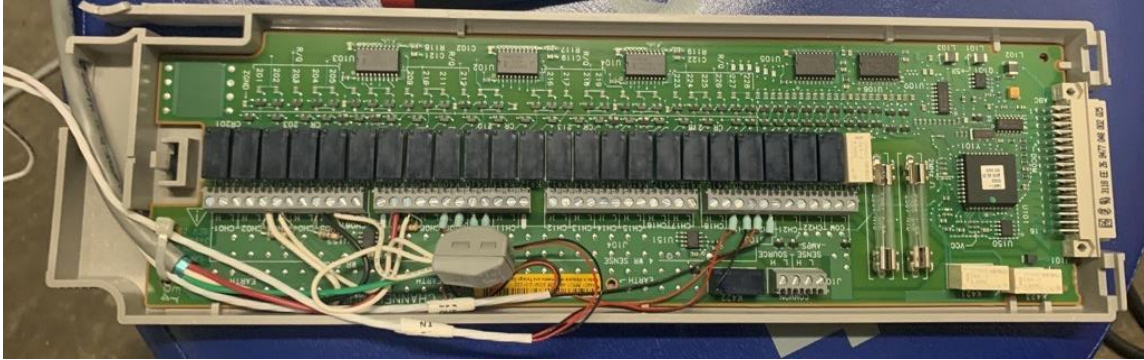


Figure 2-5 Agilent Data Card for RTD and Pressure Readings

$$V = IR \quad (11)$$

Ohm's law is shown in Equation 11 where V is the voltage, I is the current and R is the resistance. The 4-20 mA output signal from the pressure sensor scales linearly with pressure so a linear piecewise interpolation was done to convert the voltage signal into a pressure value as shown in equation 12.

$$P_{measured} = \frac{V_{measured} - I_{LowEnd} * R}{I_{HighEnd} * R - I_{LowEnd} * R} * P_{FullScale} \quad (12)$$

$V_{measured}$ is the measured voltage from the pressure sensor, I_{LowEnd} is the low end of the resolution of the sensor which is 4 mA, $I_{HighEnd}$ is the high end of the resolution of sensor which is 20 mA, R is equal to the 560 ohm resistor that was used to help convert the signal and $P_{FullScale}$ is equal to the full scale of the pressure sensor which varies from 50 psi – 200 psi depending on the sensor.

The test unit used described in this section was referred to as the Heat Quantification Unit and the purpose of the testing was to quantify the total heat loss of the hot liquid loop. The variables used to calculate \dot{q}_{HLL} and the measurement method used are shown in Table 2-1. Figure 2-6 shows the locations of the instrumentation used in this heat quantification experiment. The heat quantification unit was placed in a 90°F ambient thermally insulated test chamber. The unit went through its normal operation cycles with no interference to the normal cooling algorithm. The setpoints were 37°F in the fresh food, 0°F in the freezer and 29.5°F in the convertible drawer.

Variable	Description	Measurement Method
h_{in}	Enthalpy at the inlet of the hot liquid loop	Temperature and pressure measurements
T_{in}	Temperature at the inlet of the hot liquid loop	4-wire RTD
P_{in}	Pressure at the inlet of the hot liquid loop	Omega PT200 pressure transducer
h_{out}	Enthalpy at the outlet of the hot liquid loop	Temperature and pressure measurements
T_{out}	Temperature at the outlet of the hot liquid loop	4-wire RTD
P_{out}	Pressure at the outlet of the hot liquid loop	Omega 50 differential pressure transducer and Omega PT200 pressure transducer
\dot{m}	Mass flow rate of refrigerant	Calculated using regression that uses P_{out} and P_{suct} as inputs
P_{suct}	Suction pressure of compressor	Omega PT100 pressure transducer

Table 2-1 Variables and their measurements methods used in Heat Quantification of Hot Liquid Loop Experiment

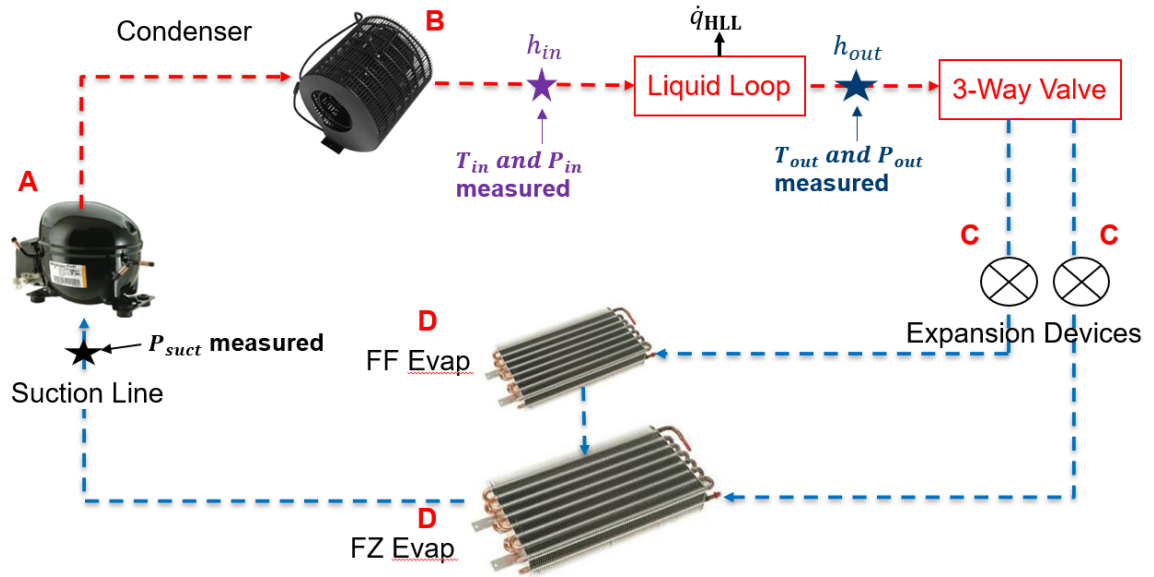


Figure 2-6 Schematic showing measurement locations of the sensors

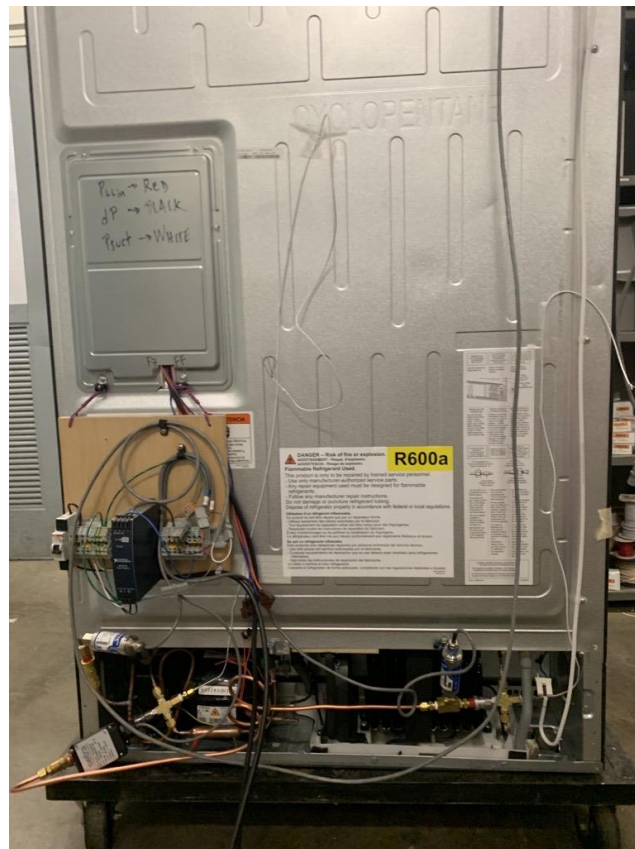


Figure 2-7 Back view showing instrumentation used on the Heat Quantification

Unit

2.2 Forward Heat Leak Calorimeter System

To determine the fraction of heat dissipated into the compartment, a test unit was placed in a forward heat leak calorimeter system which was set up to capture the amount of heat that was being removed from the cabinet by the evaporators. The forward heat leak system used in this study is similar to the one constructed in a previous study conducted by Berghuis (2020) on the experimental evaluation of heat leak and convective heat transfer in a household freezer. The general construction of the system remained intact as most of the sealed system components were the same such as the compressors dryer, accumulator etc. as shown in Figure 2-8. A benefit with the forward heat leak calorimeter system was the capability of controlling the cooling capacity of the FF and FZ compartment by use of TXV which controlled how much refrigerant was entering the evaporators. Additional information regarding the construction of the forward heat leak system can be found in the referenced study.

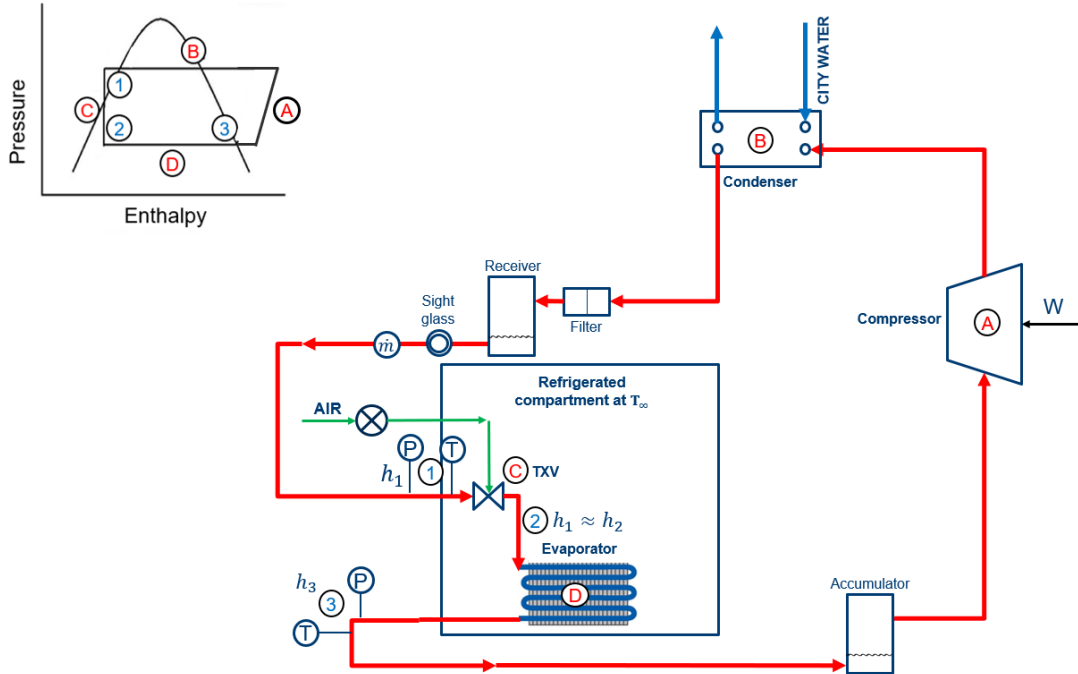


Figure 2-8 Schematic of instrumented forward heat leak calorimeter (Berghuis, 2020)

The heat that must be removed from the cabinet by the evaporators is due to the heat leak of the compartment of interest. The procedure was to obtain a baseline heat leak value prior to turning on the anti-sweat component of interest, then activating the component and observe the difference in the calculated heat leak value. The difference between the baseline and the new value should tell how much additional heat the operation of an anti-sweat component contributes. In normal operation of a refrigerator/freezer unit, the compressor usually oscillates between the on/off states based on predetermined compartment states. Stable compartment temperature control would ensure consistency in the heat leak value calculations, so a configuration where there is a dedicated compressor for the fresh food and freezer/convertible drawer compartment would

be ideal so the compressor can never turn off and keep the respective compartment at the same temperature indefinitely.

Heat leak is measured by calculating the difference in enthalpy between the inlet of the evaporator (directly before the expansion device), and the outlet of the evaporator. The enthalpy for the inlet of the evaporator had to be measured before the expansion device because the refrigerant becomes a low pressure, two-phase mixture after exiting the expansion device and obtaining an enthalpy would be a difficult process without knowing the vapor quality. Since the expansion is an assumed isenthalpic process, the enthalpy at both locations should yield the same value. Refrigerant that enters the expansion device should be high pressure subcooled liquid and will be low pressure superheated vapor at the outlet, so pressure and temperature are all that is needed to define states.

2.3 Household Refrigerator-Freezer used in Forward Heat Leak Testing

The experimental refrigerator-freezer unit that was used for this study was a dual evaporator single damper model. Figure 2-9 shows the test unit connected to the forward heat leak system. Holes were drilled on the right side of the case to connect the evaporators in both compartments to the forward heat leak system shown in Figure 2-10. To address the air/heat leakage created from introducing holes in the case, the copper and air lines were fed through the case and foamed in to cover the gaps.

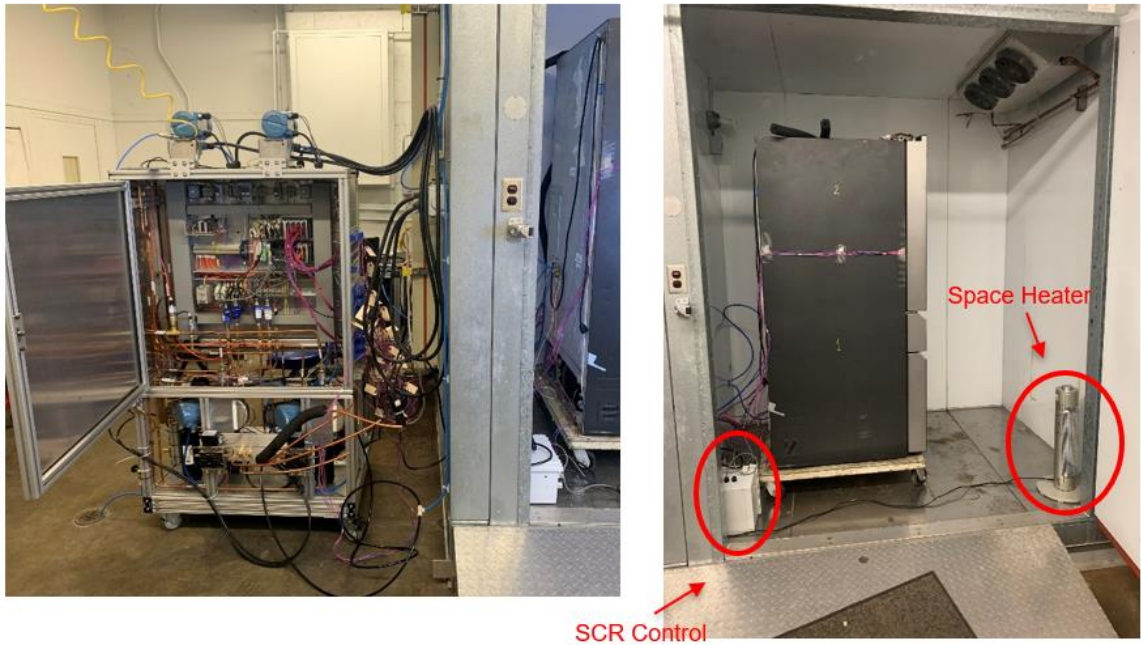


Figure 2-9 Forward Heat Leak System Connected to Household Refrigerator
used for this study

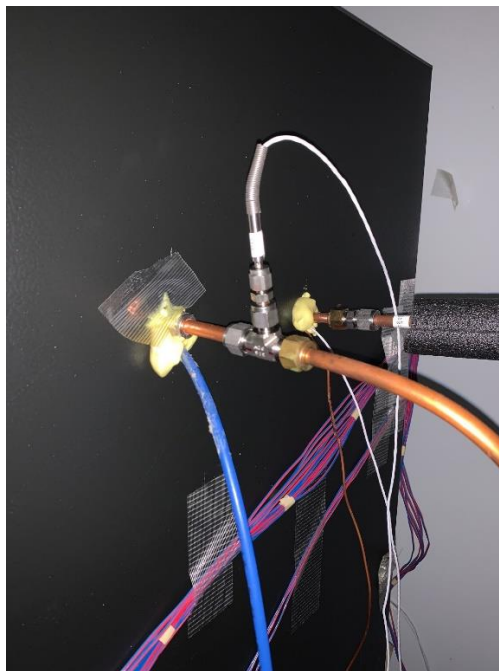


Figure 2-10 Copper Tubes from Forward Leak Calorimeter System fed from side
of the case into the FF compartment

NPT fittings and pipe unions were used throughout the unit. Teflon tape was wrapped around the threading of the NPT fittings to improve the seal of unions to ensure no leaks occurred.

Temperature and pressure were recorded at the inlet and outlet of the evaporators. Insulation was wrapped around the suction line of the evaporators shown in Figure 2-11, to minimize the heat gain as the refrigerant traveled to the evaporator. The fans in each respective compartment were turned on for 100% of the testing to ensure stable temperatures. The data collected was processed by the National Instruments modules in the data acquisition system and then displayed/graphed in a LabView executable. The unit was placed in a thermally insulated chamber where the ambient was maintained to 90°F by a space heater.

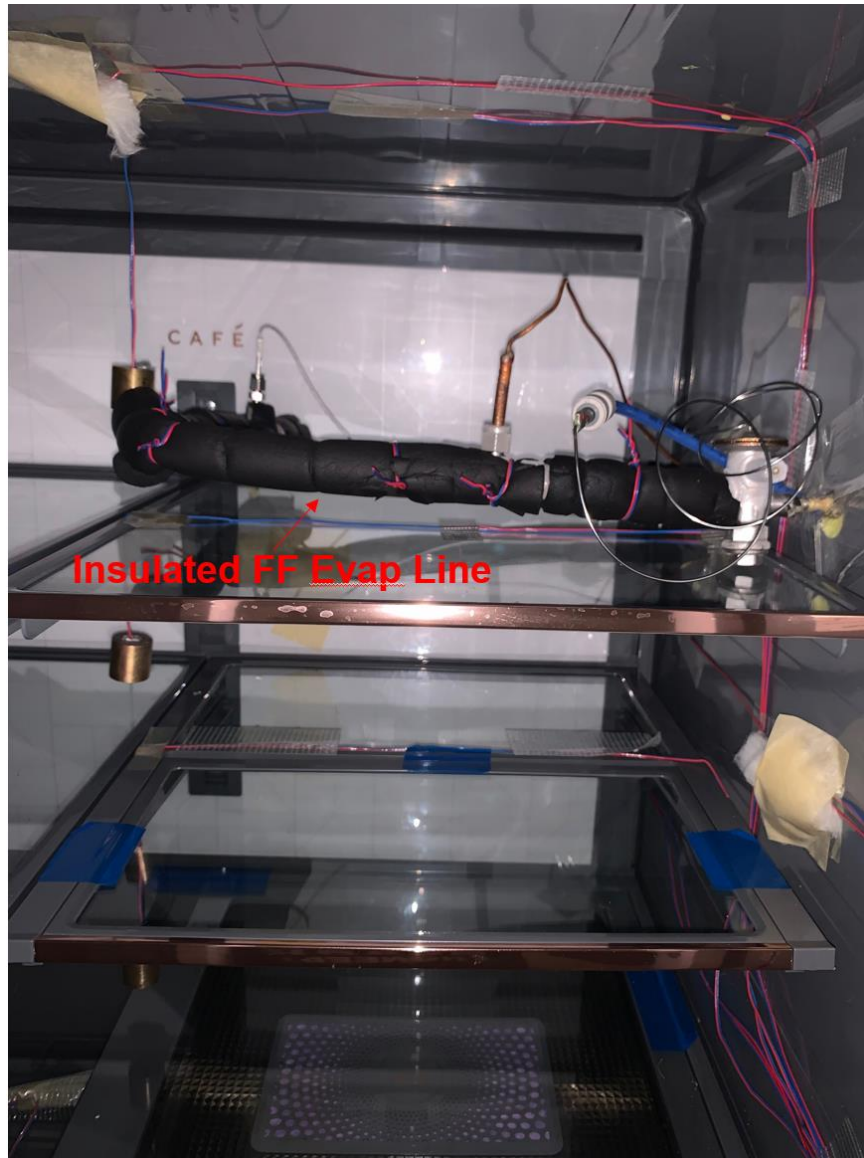


Figure 2-11 Insulated copper FF evap suction line in test unit used in Forward Heat Leak calorimeter system

The experiment mimics the operating conditions in which the Department of Energy (DOE) uses to determine the energy usage of a product and what the appliance industry has defined as the nominal setpoint. The setpoint temperature for the fresh food compartment is 37 °F, the freezer is 0 °F, and the convertible

drawer is 29.5 °F. This is the nominal test point used by the DOE and the appliance industry for energy use tests.

2.4 Proportional Integral (PI) Control of Different Components & LabView

Interface

To record the heat leak values in the Forward Heat Leak calorimeter with a high level of certainty, stable temperatures for the three refrigerated compartments for at least five hours is desired. There are three outputs that directly affect the temperature of each compartment: fan speed, compressor speed, and the opening of the thermostatic expansion valve (TXV).

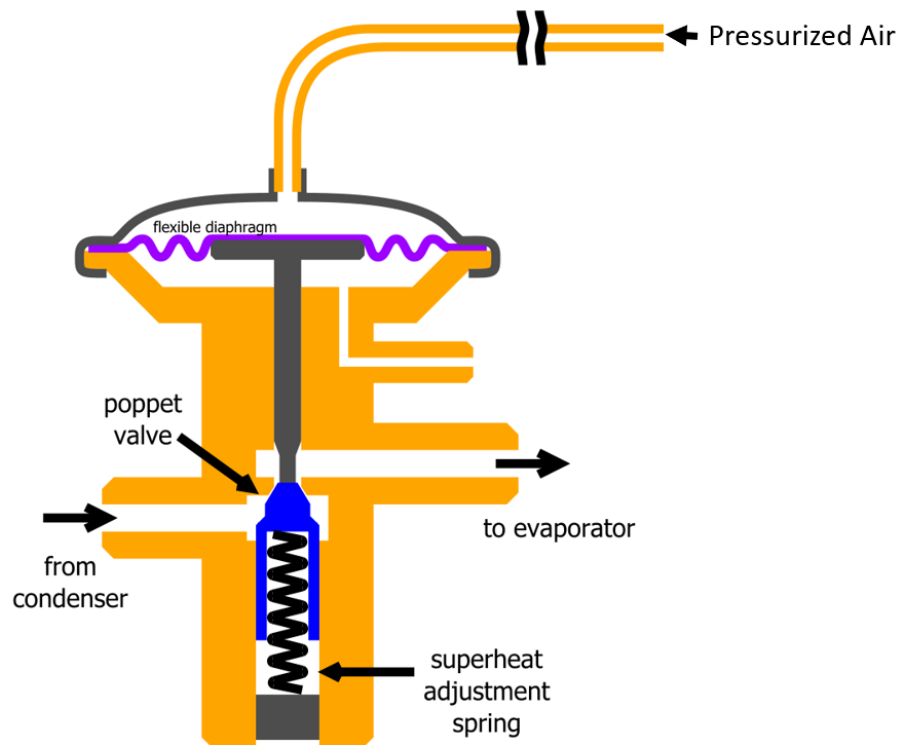


Figure 2-12 Diagram showing Thermostatic Expansion Valve construction in

FWHL system

The thermostatic expansion valve shown in Figure 2-12 acts as a metering device for the system and controls the amount of refrigerant entering the evaporator. Normally the flexible diaphragm of the TXV is connected to the outlet of the condenser and the amount of superheat on the evaporator drives the opening of the expansion device via a thermostatic element, such that an increase in superheat creates an expansion of the thermostatic charge which in turn forces the valve to open by exerting a pressure on the diaphragm. For this experiment, the thermostatic charge bulb was replaced with a direct line to compressed air to manually control the opening of the valve and thus the amount of refrigerant entering the system, thus having direct control of the cooling capacity. As air is sent to the flexible diaphragm, the valve opening increases which allows more refrigerant to flow through to the evaporator.

A LabView program was written to read and export the data from the instrumentation as well as provide direct control of the compressor speed, TXV opening percentage, and the opening percentage of the convertible drawer damper. With multi-hour temperature stability for each compartment needed for the experiment, manual operation of the process variables would be tedious and inefficient. Automatic control where the system would maintain the desired setpoint without human interference was ideal, so a Proportional Integral (PI) controller was established with the relevant outputs. A PI controller is used to control an output and bring a process value to a desired setpoint. It works by calculating how far away the current value is from the setpoint value and using that error to proportionally adjust the output of the process variables. Figure 2-13

shows the LabView program interface that was used to control the Forward Heat Leak calorimeter system.

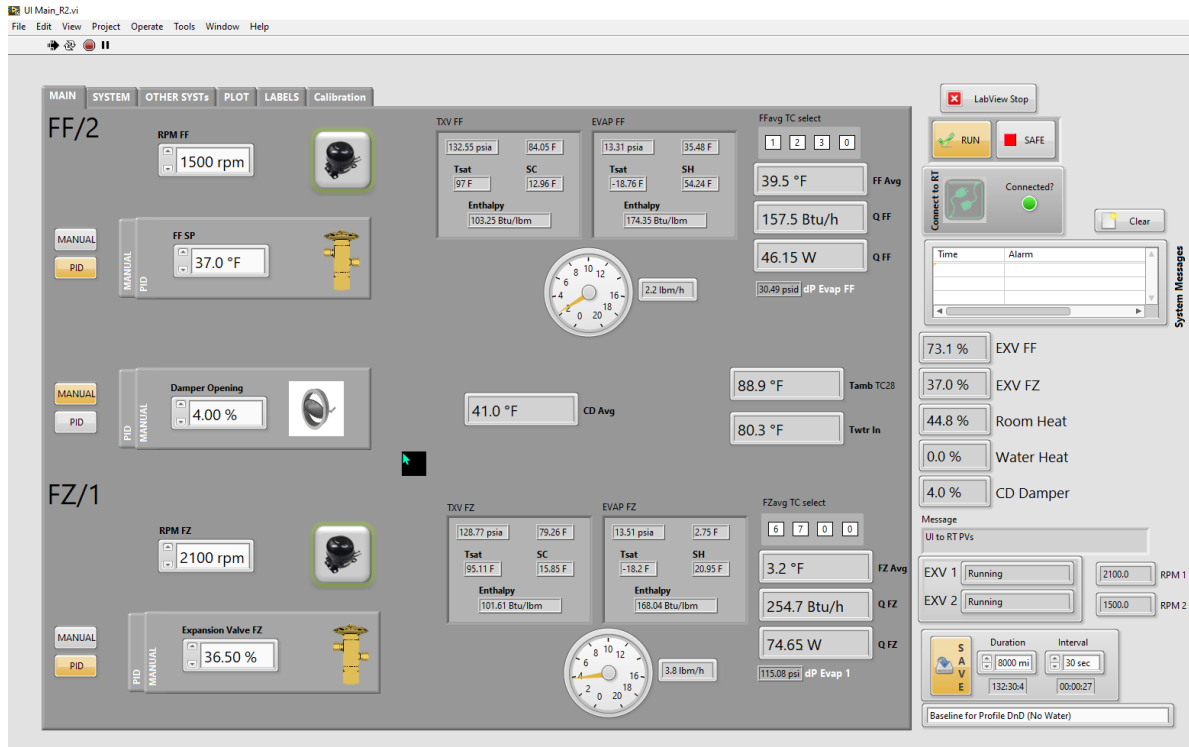


Figure 2-13 LabView Interface of Control and Measured Parameters for Forward Heat Leak System

As mentioned in the beginning of this section, there are three different outputs (fan speed, TXV opening, compressor speed) that affect the compartment temperature. While simultaneous automated control would be possible for all three, the continual adjustments between variables would fight against each other and be counterproductive. Instead, the compressor speed was fixed as the system response for varying this component was relatively long as well as having a constant shift of compressor frequency would create significant variation on the mass flow which should be avoided. The fan speed

was also chosen to be fixed as there was not substantial impact to compartment temperature in certain speed ranges and would not be a useful process variable in continuous control. The TXV opening was chosen to be the output for the compartment temperature as none of the issues stated prior applied. Multiple PI controllers were tuned to maintain a system response characterized by limited variation, such as for the TXV opening, damper opening, space heater power output and hot water temperature.

The PI tuning process was the same for each of the components. Figure 2-14 shows the temperature response of the forward heat leak system during the tuning of the TXV for the FZ compartment. Referencing the figure, the unit is initially in a stable data region where the temperature in the FZ compartment does not vary more than 0.2°F for over 1 hour. A disturbance is introduced to the system where the TXV opening percentage is changed by a fixed amount. In the case shown, the opening percentage was increased from 4% to 5%. The data will eventually restabilize and that is when the testing is complete. Analyzing the system's response to the disturbance (in this case the TXV opening % change) allowed the calculation of the "gain coefficients" to implement into the PI control and maintain automatic control of various system parameters. The gain coefficients are the values that determine how much the system adjusts the output over time to reach the desired setpoint.

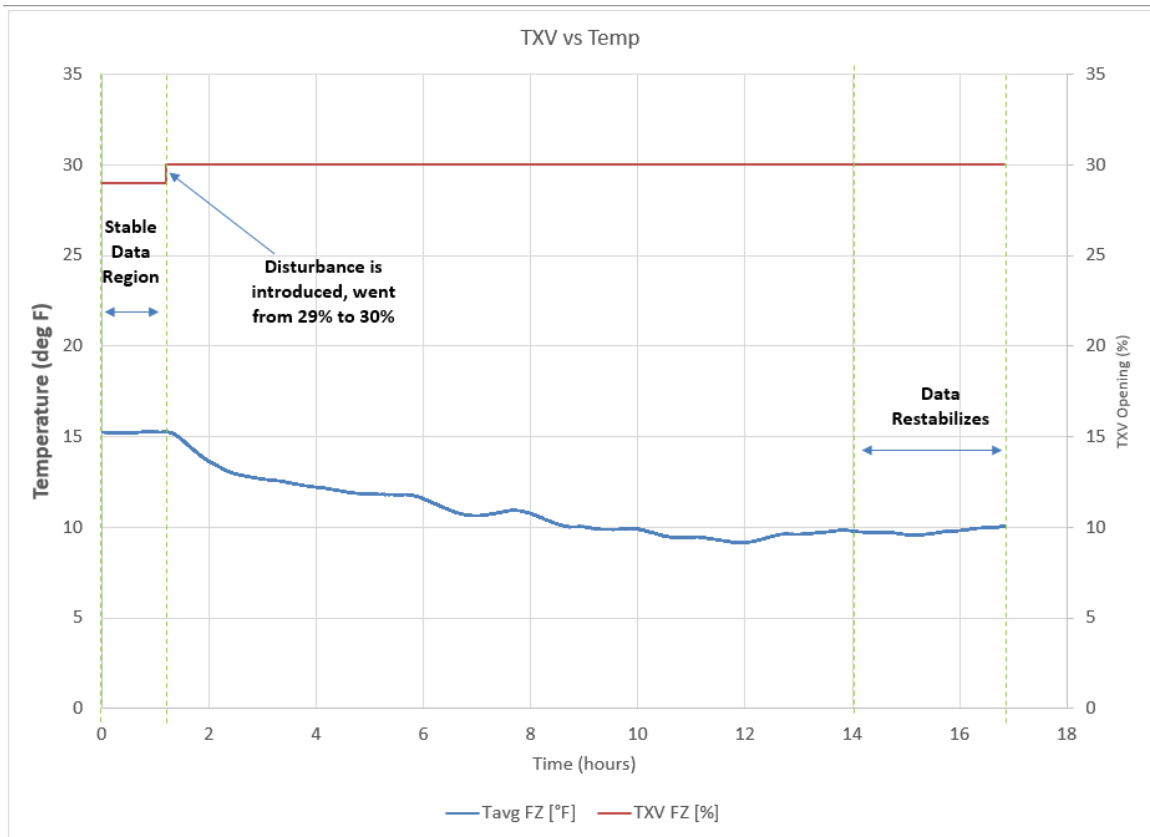


Figure 2-14 Temperature illustrating the PI tuning process for the TXV in the freezer compartment

The process values in this Forward Heat Leak Experiment were controlled by different means. A silicon-controlled rectifier (SCR) was used with the space heater to control it with a 4-20 mA signal. The TXVs were connected to a pneumatic pressure regulator that controlled how much air was being sent to the diaphragm within the TXV, and the regulator was also controlled with a 4-20 mA signal. The damper opening was controlled with a 0-12 VDC signal. Using the TXV as an example, to tune the TXV PI controller, stability at a baseline process value (compartment temperature in this case) is required then a disturbance to the output (TXV opening) will show how long it takes the system to react to the

output change and the gain factors the PI controller can be determined. A table summary showing the variables that were PI controlled is shown in Table 2-2.

Process Value	Output	Control
Test Chamber Temperature	Heater Current	4-20 mA electrical signal
FF Temperature	TXV Opening %	Regulated air controlled by 4-20 mA electrical signal
FZ Temperature	TXV Opening %	Regulated air controlled by 4-20 mA electrical signal
CD Temperature	Damper opening %	Electrically controlled damper by 0-12 VDC signal
Water Inlet Temperature	Immersion Heater Current	4-20 mA electrical signal

Table 2-2 Summary of PI controlled variables and their respective process variables

2.5 Modeling Heat Loads of Anti-Sweat Components in Forward Heat Leak (FWHL) System

The FWHL system provided the capability to determine the amount of heat from the anti-sweat components which entered the cabinet. The anti-sweat components observed in this study were four different electrical heaters (shown in Table 2-3 and the hot liquid loop. The total heat dissipated from the electrical heaters was known since these heaters were rated at a specific wattage output and this number is the same as the total rate of heat produced by the anti-sweat components (heat load). The First Law of Thermodynamics dictates that in a

closed system at steady state, the heat output is equal to the work put into the system, which in this case the heater wattage. To test an anti-sweat component, the component of interest was turned on and the change in heat leak values was recorded from the forward heat leak experiment. The change in heat leak between when the anti-sweat component is turned on and off shows the portion of the heat load that enters the refrigerated compartments.

Heater Name	Heater Wattage (Heat Load)
Articulating Mullion Heater	11 W
Door-In-Door Heater	10.5 W
Ice Dispenser Heater	1.25 W
Icebox Gasket Heater	5 W

Table 2-3 Rated heater wattages of the electrical heater anti-sweat components

In actual operation, the heaters are not on one hundred percent of the time as they are tied to the specific ambient humidity conditions however for the purposes of this study the heaters were turned on at 100% duty cycle to observe the maximum effect from these components as these refrigerator appliances are generally designed to address worst-case ambient sweat conditions.

The hot liquid loop (HLL) is a two-phase refrigerant mixture and therefore required a different approach to obtain the heat load values as described in section 2.1. While the section describes the method to obtain the total heat load from the HLL, this component still needs to be modeled within the FWHL system

to be able to determine the fraction of heat entering the cabinet. Recreating the heat load with a R600a refrigerant hermetic system would be the most representative in theory however, it would be bringing many complications. A major issue being the ability to manually adjust to desired inlet conditions as well as the extraction of information. A new compressor, expansion device and heat exchangers would have to be utilized as well as an appropriate method to control the inlet conditions. While temperatures and pressures can be recorded at any location, if the refrigerant is underneath the vapor dome at any point of the process, it would not be possible to extract an enthalpy value with just two parameters (temperature and pressure). Also, a mass flow meter becomes highly inaccurate in the presence of a two-phase mixture.

Instead, water was chosen as the fluid to recreate the heat load of the HLL. With the temperature range of the study, water will be a single-phase fluid so the enthalpy can be calculated at any point with a known temperature, pressure, and fixed mass flow rate. A water pump controlled by a DC motor drive controlled the flow of water and a 2000W Watlow immersion heater controlled the temperature. A schematic of the hot water system is shown in Figure 2-15. While the specific heat capacities between Isobutane and water are different, there is not a large temperature difference across the HLL, so the impact of the difference was assumed to be negligible. Water treatment was added to the tank to deter bacteria growth and rust formation within the steel hot liquid loop. Figures 2-16 and 2-17 show the hot water system and the interaction to the forward heat leak test unit.

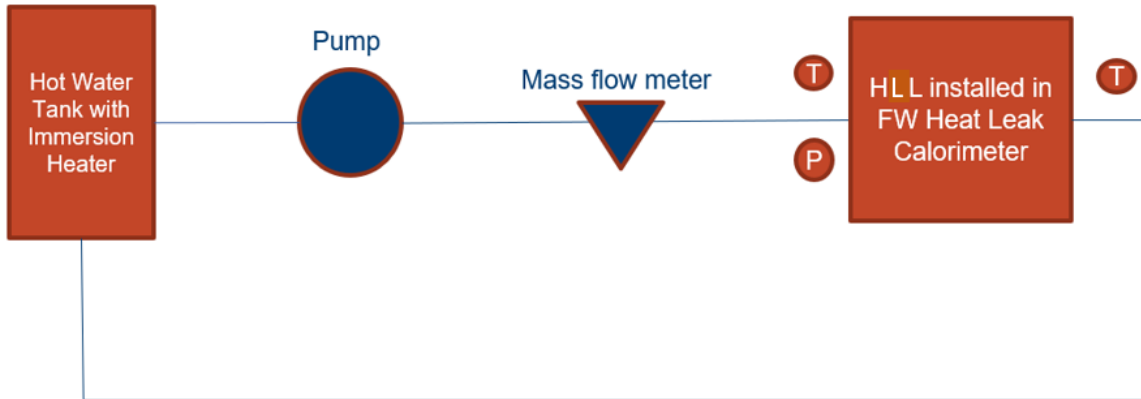


Figure 2-15 Schematic of hot water system used in forward heat leak

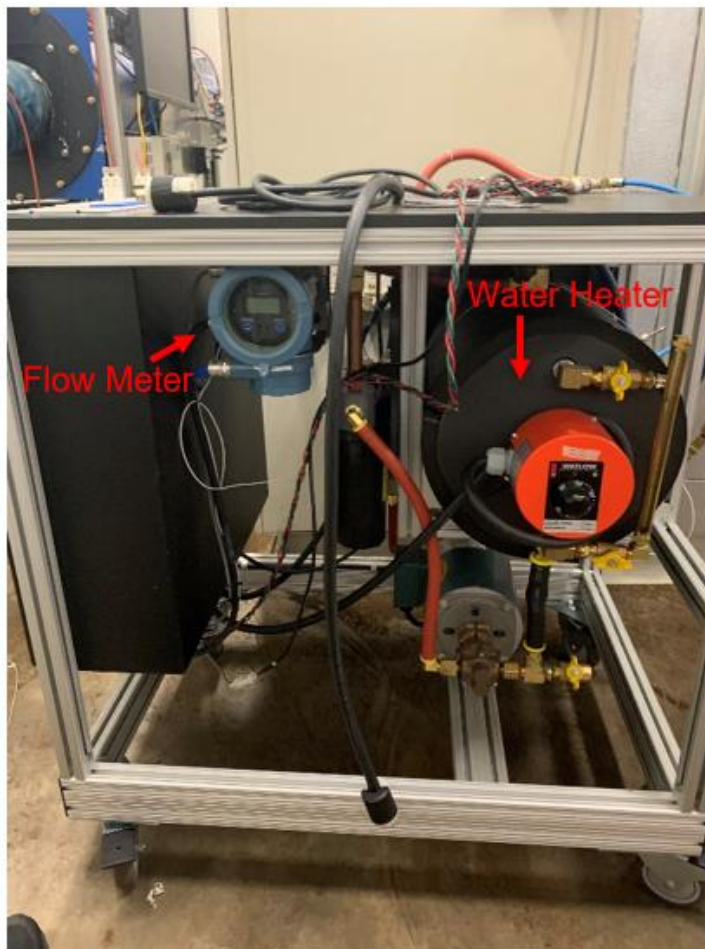


Figure 2-16 Photo of hot water system used in forward heat leak

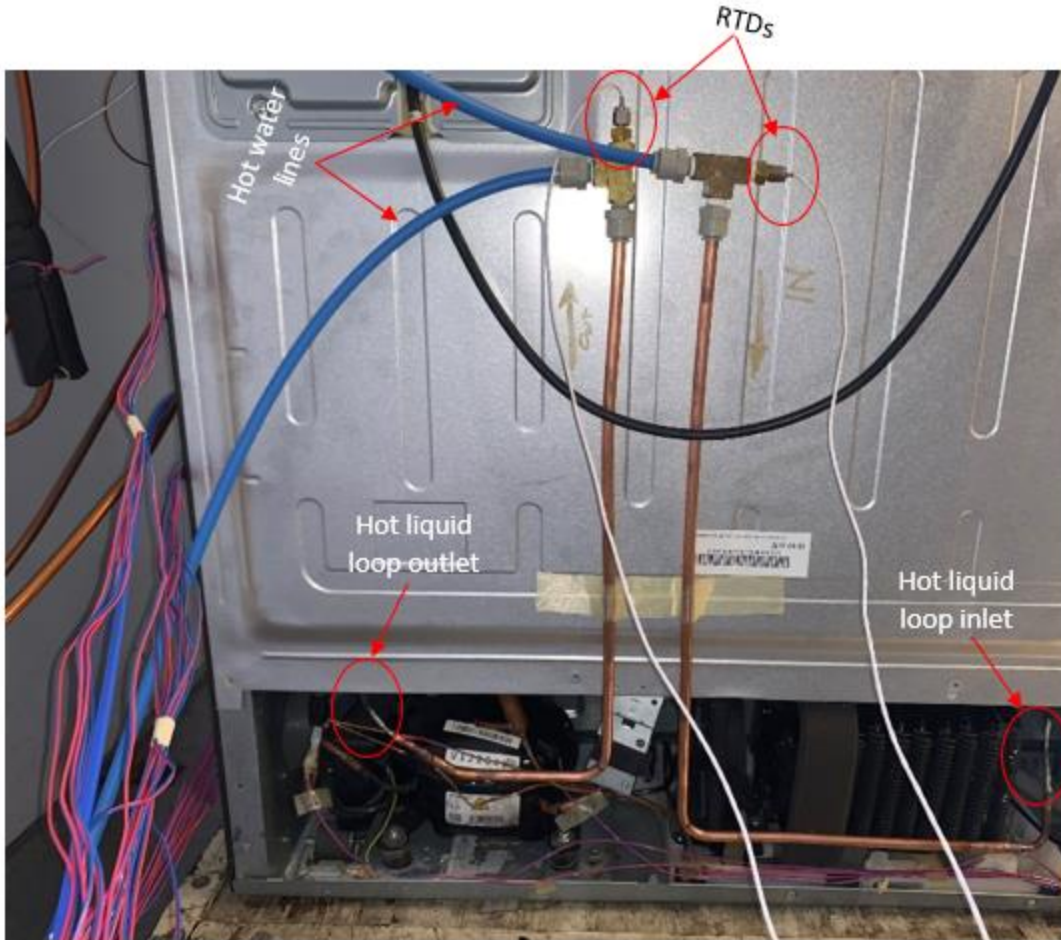


Figure 2-17 Photo of hot water system entering in forward heat leak system test unit

With the heat load of the HLL, \dot{q}_{HLL} , known from the experimental procedure described in section 3.1, the same load can be recreated with the hot water system (referred to as hot water loop in this paper) so $\dot{q}_{HLL} = \dot{q}_{Water}$.

$$\dot{q}_{water} = \dot{m} * C_p * (T_{in} - T_{out}) \quad (13)$$

The water pump is controlled by a Volts to Direct Current (VDC) signal motor and the immersion heater for the water temperature has a Silicon Controlled Rectifier (SCR) installed so the effort of the heater can be adjusted

accordingly. The mass flow meter was a CM025 model from Emerson solutions. With the specific capacity of water being approximately constant, the heat load of the water can be controlled with relatively large amount of precision. PI control was established for the hot water system with the water temperature being the process value and the mass flow rate being a fixed value. The variables used to calculate Q_{water} and the measurement method used are shown in Table 2-4.

Variable	Description	Measurement Method
\dot{m}	Mass flow rate of hot water system	Micro Motion CMF-10 Coriolis mass flow meter
T_{in}	Temperature at the inlet of the hot water system	4-wire RTD
T_{out}	Temperature at the outlet of the hot water system	4-wire RTD

Table 2-4 Variables and measurement methods used to control hot water system

heat load

3 MODELING PERFORMANCE OF REFRIGERATOR WITH AMESIM

3.1 Background on AMESIM Software

The goal of this study is to determine the fraction of heat entering the cabinet from various anti-sweat components and understand how that additional heat affects the energy usage and general thermal performance of the unit. The method to obtain the rate of heat added to the refrigerated compartment has been previously described and the following sections will address analyzing the effect on energy usage. AMESIM, which stands for Advanced Modeling Environment for performing Simulations of engineering systems, was used to develop a model of the refrigerator/freezer. The software uses one-dimensional simulations and utilizes bond graph theory to model real life systems. A Bond graph, in short, is a graphical representation of a physical dynamic system that uses “bonds” to link together components. An example of bond theory being used to model a simple mass-spring-damper system is shown in Figure 3-1.

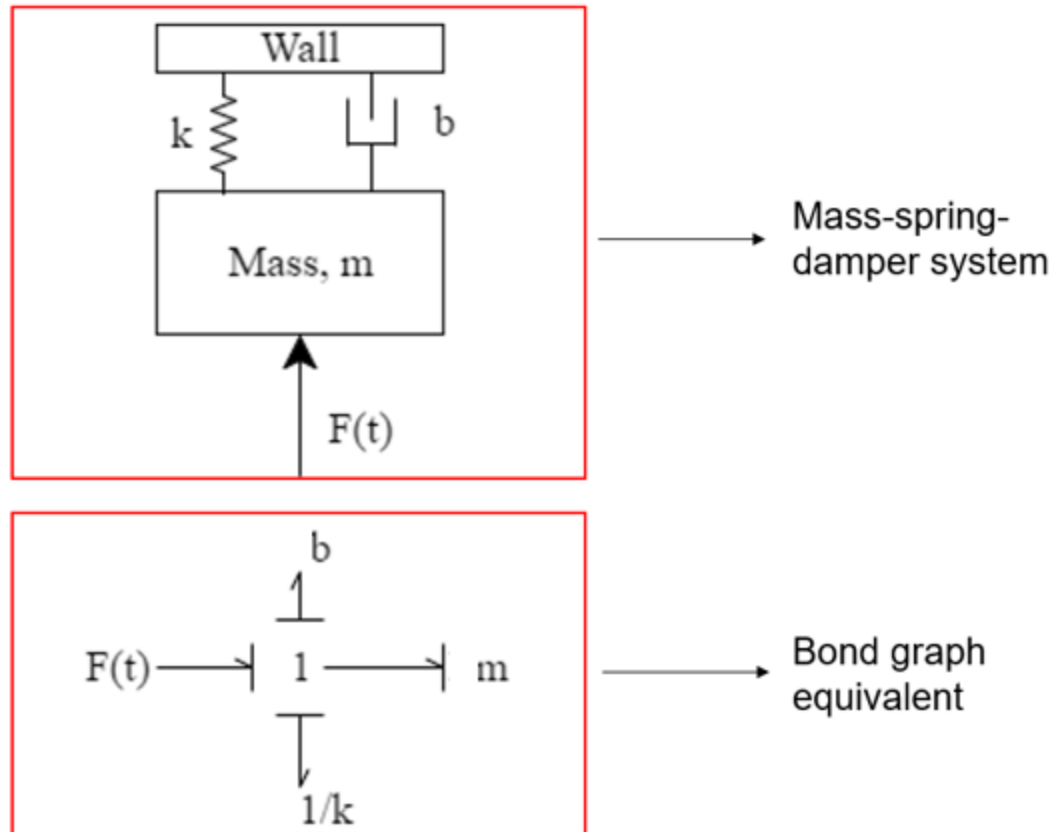


Figure 3-1 Schematic showing simple mass-spring damper system modeled using bond graph theory

To create a simulation model for a system, a set of libraries are used that contain pre-defined and user defined components. These components model different physical domains such as heat exchangers, ambient conditions, pipes, etc. Accurately describing the system with the appropriate components and connecting them in proper relation to each other is a fundamental aspect of AMESIM models. An example of a refrigerator wall being modeled in AMESIM is shown in Figure 3-2. The components used in the model are connected in a manner that is representative of the physical system and the parameters such as

temperature and surface convection are user defined and dependent on the system that is being modeled.

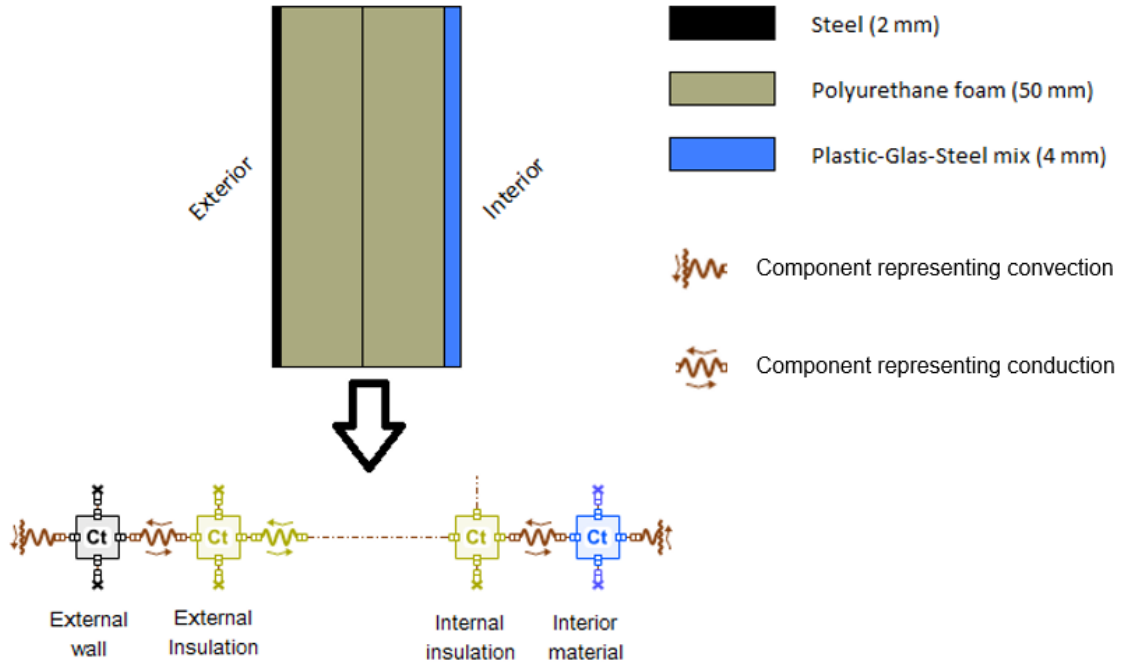


Figure 3-2 Example of AMESIM being used to create thermal model of a refrigerator wall

3.2 Construction of Household Refrigerator/Freezer Model in AMESIM

The experimental unit used for this study was a dual evaporator model (one in the FF and FZ compartment each) with a damper that connected the freezer to the convertible drawer and supplied its cooling. It was a French door model with the ice and water dispenser being located on the left-hand door. The volumes of the compartments are shown in Table 3-1.

Compartment	Internal Volume (ft³)
Fresh Food	15.62
Convertible Drawer	3.62
Freezer	8.57

Table 3-1 Internal Volumes of refrigerated compartments of experimental study unit

The entire system modeled in AMESIM is shown in Figure 3-3. The following sections will describe how each of the components were defined and their purpose in the overall model of the system. The blue dashed lines are the bonds that link the supercomponents together and is supposed to mimic the flow path of the refrigerant. The red dashed lines are generic bonds that link any two items together and purple was used for the FF and FZ fan airflow. The supercomponents are the labeled elements such as the condenser, compressor, etc. that will be explained in further detail in the following sections.

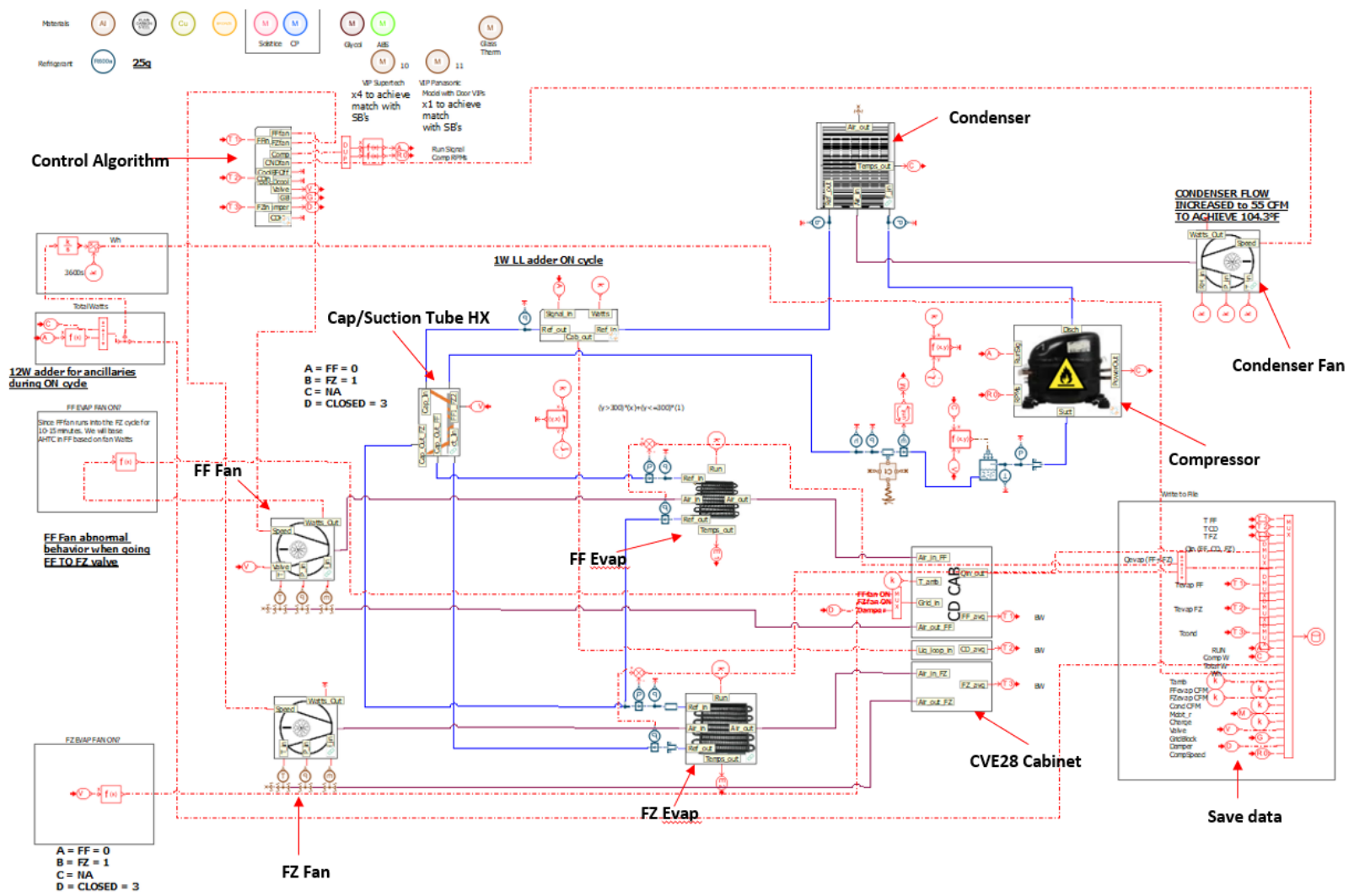


Figure 3-3 System Level View of test unit Refrigerator Unit Modeled in AMESIM

The material properties in this simulation were defined based on the actual construction of the test unit. Well-known material properties were readily available in the AMESIM library. The materials that already had definitions from AMESIM were pure aluminum, plain carbon steel, copper, and bronze. The default AMESIM library provides material information for a large range of temperature that covered the range of this application.

The vacuum panel, plastic liner material (ABS) and glass used on the shelves inside the unit were user defined values based on information provided by the makers of said material. The thermal insulation foam's thermal conductivity (k value) varies with its temperature and a linear regression relation of thermal conductivity as a function of temperature is provided by the supplier of the material. A table summarizing the materials used in this study is shown in Table 3.1. The refrigerant used in the unit and model is Isobutane which was readily available in the AMESIM database, and the modified Benedict-Webb-Rubin was used as the equation of state.

Material	Use In Model	Thermal Conductivity @ 25°C (W/m K)
Pure Aluminum	Evaporator Fins	238
Plain Carbon Steel	Outer Case	60.8
Pure Copper	Tubes carrying refrigerant	402.2
Commercial Bronze	Brass Weights (with thermocouple embedded)	50.94
ABS	Plastic Liner	.2
Cyclopentane Foam	Thermal insulation foam	.018
BK7 Glass	Glass on shelves	1.1
VIP (Panasonic)	Vacuum Insulation Panel	.0023

Table 3-2 Materials used in AMESIM model and their thermal conductivities

The thermal circuit goes as follows; convection occurs from the ambient air on the steel outer case in which the heat then conducts through the case and depending on the wall the next component in contact will be the thermal insulation foam (cyclopentane) and possibly also a Vacuum Insulation Panel (VIP). A VIP is a rectangular panel that provides a lower thermal conductivity than foam and is used to improve the insulation capabilities of the cabinet. The heat then conducts through the plastic liner which is defined as ABS in the model

and is the internal white walls that the user sees when looking into any of the compartments. There is then convection off the plastic liner wall into one of the respective cooled compartments. The thermal response in terms of warming and cooling rates of the unit is affected by the glass shelves and plastic baskets present in the compartment as these affect the thermal mass in addition to the surrounding walls/foam. A thermocouple embedded into a brass weight placed in the geometric center of the compartment is used to capture the average air temperature of the respective compartment.

3.3 Creation of Supercomponents used in AMESIM Model

As previously mentioned, the compressor, condenser, capillary tubes, compartment fans and evaporators are the major components in the hermetic system of a refrigerator and are all modeled in AMESIM as supercomponents. The intent of the supercomponents is to reflect the behavior of the physical component by supplementing the model with real test data and correlations. Each of the components and how they were modeled will be explored in the following sections.

3.3.1 Modeling of Compressor as Supercomponent in AMESIM

A detailed view of the compressor supercomponent is shown in Figure 3-4. The compressor is responsible for pressurizing the low-pressure vapor coming from the evaporator and discharging high pressure vapor to the condenser. The parameters of the compressor that affect the energy

consumption of the refrigerator are the mass flow rate, electrical power consumption of the compressor, and the cooling capacity of the refrigerant are all calculated as a function of suction and discharge pressures. The correlation used in the AMESIM model was a least squares regression polynomial which was generated using experimental data from compressor calorimeter testing.

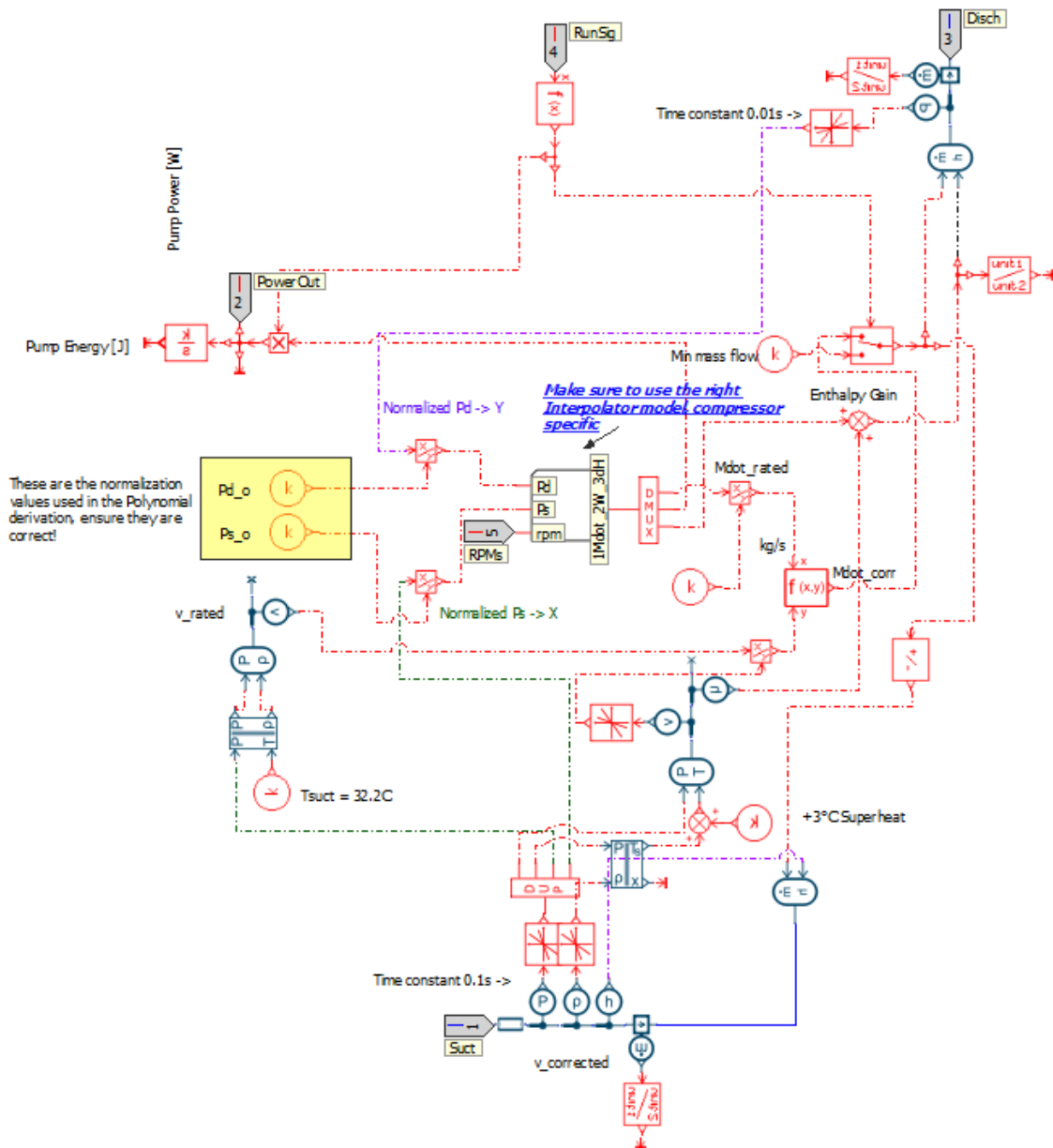


Figure 3-4 Compressor supercomponent modeled in AMESIM

The Air-Conditioning, Heating, and Refrigeration Institute STANDARD 540-215 references the method in which manufacturers are expected to report the compressor power input, mass flow rate and refrigerating capacity and was used as a guide for the creation of the correlation. While the standard uses suction and discharge saturation temperature in the correlation (mostly to have a consistent reference point between different refrigerants), for the purposes of this experiment the pressures were chosen instead as the instrument uncertainty with pressure sensors when compared to a RTD was considerably less. A total of 11 test points were obtained at a specified compressor frequency ranging from 43 Hz to 150 Hz. The suction temperature was fixed at 90 degrees F while the suction and discharge pressures were varied at the different test points. Three polynomials were created using the suction and discharge pressures as the variables and each providing either the mass flow rate, compressor power or change in enthalpy as the output. The polynomial equation will be in the form shown in Equation 14,

$$X = C_1 + C_2 * P_s + C_3 * P_d + C_4 * P_s^2 + C_5 * (P_s * P_d) + C_6 * P_d^2 + C_7 * P_s^3 + C_8 * (P_d * P_s^2) + C_9 * (P_d * P_s^2) + C_{10} * P_d^3 \quad (14)$$

where C_1 through C_{10} are the regression coefficients calculated from the calorimeter data. The coefficients will change when observing different sets of data (for example when comparing different compressor frequencies) or looking at different outputs (mass flow rate, compressor wattage, or capacity). P_s is the suction pressure and P_d is the discharge pressure. X is one of the three different

outputs of interest, and depending on the output, the correct set of coefficients must be used.

As mentioned previously, test points were taken at varying compressor frequency ranging from 43-150 Hz. If the properties of a frequency were needed at a speed that was not tested, a linear interpolation was performed between the closest high and low value. The sub model used to interpolate to a requested angular velocity (RPM) value is shown in Figure 3-5. An input RPM as sent in from the model is read by the function and an interpolation is performed between the two closest data points.

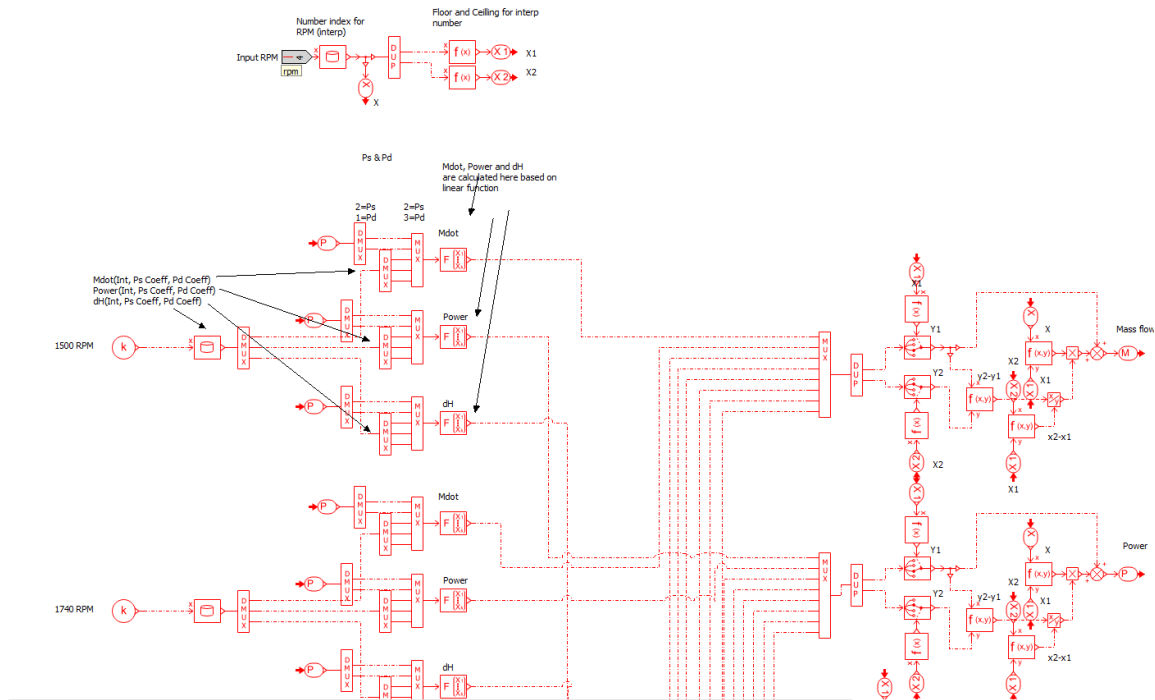


Figure 3-5 Compressor angular velocity, cooling capacity, and compressor power interpolator modeled in AMESIM

3.3.2 Modeling Heat Exchangers as Supercomponents in AMESIM

Three heat exchangers were modeled: the condenser, fresh food (FF) evaporator and the freezer (FZ) evaporator. The construction between the three supercomponents are similar but each with their own subtle differences. The creation of the fresh food evaporator will be explained first and the differences between the others will be explored afterwards.

A photo of the fresh food evaporator is shown in Figure 3-6 which is a one bank, nine-pass evaporator configuration.

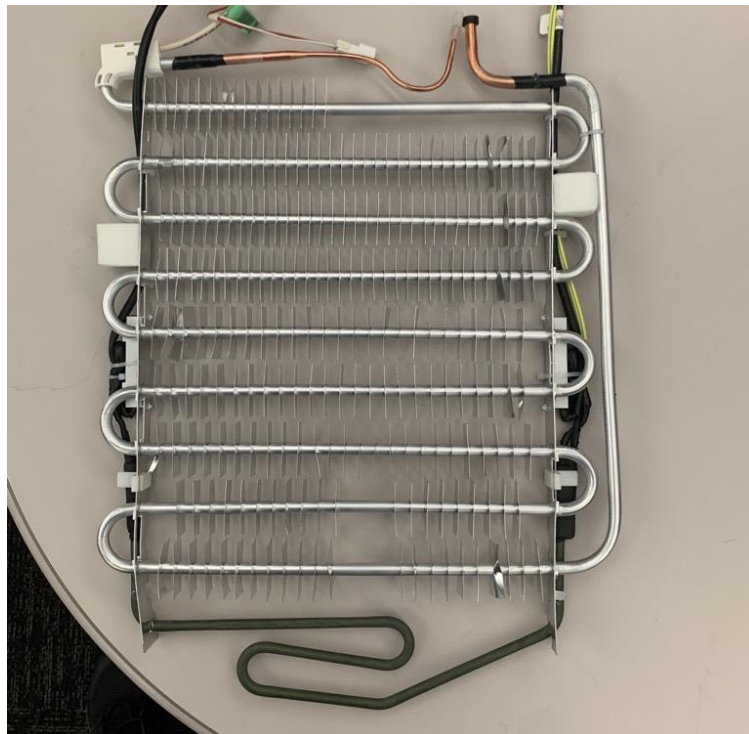


Figure 3-6 Fresh Food Evaporator

A detailed view of the fresh food evaporator supercomponent is shown in Figure 3-7.

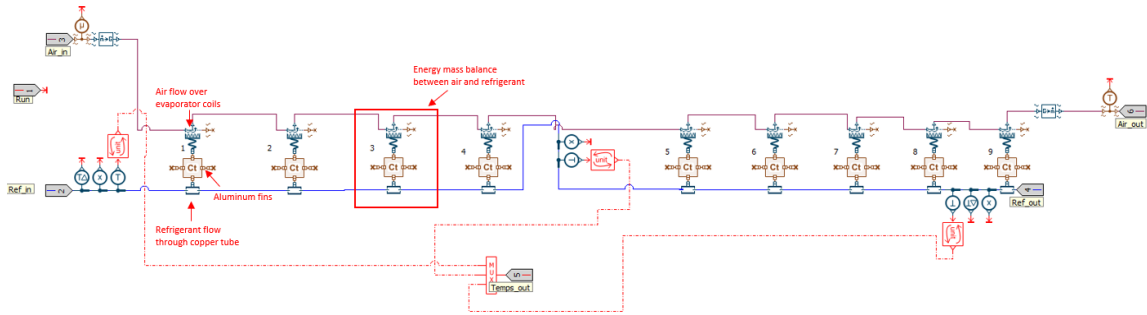


Figure 3-7 AMESIM Model of Fresh Food Evaporator supercomponent

As shown in the AMESIM model, nine elements of heat exchange are shown to model the nine-pass configuration of the evaporator. The refrigerant flowing through the tubes was modeled using established heat transfer correlations, namely Gnielinski for the Nusselt number correlation for single phase and Mac Adams correlation for two-phase flow frictional pressure drop. The correlations for pressure drop and convection were readily available in AMESIM default library, and the most suitable relationships were chosen given this particular range of operation. The heat exchanger geometry was measured from the physical part and implemented into the model.

A slightly different process was done for the air side heat exchange as the correlation for air heat exchange was found experimentally. The values entered for the heat exchanger geometry were measured from the physical part. The coefficients used in the turbulent Nusselt number correlation were calculated from heat exchanger calorimeter testing. The test consists of having the heat exchanger in a well-insulated environment and performing an energy balance between the refrigerant and the air. The heat transfer coefficient is calculated based on how much the air temperature rises. Multiple test points are obtained

with varying air and liquid flow in which the coefficients can be extracted from a regression tool in the AMESIM model.

The condenser and the freezer evaporator were modeled with the same concept as the fresh food evaporator. The freezer evaporator is a six bank, three pass heat exchanger that uses the same air and refrigerant side correlations as the fresh food evaporator while the condenser is of a tube-fin geometry. The difference in the input for each heat exchanger is the fin configuration, tube, and pass geometry, and the heat exchange convection correlation was derived from different calorimeter testing.

3.3.3 Modeling Fans as Supercomponents in AMESIM

Three fans in this unit, the condenser fan, the fresh food fan, and the freezer fan, needed to be modeled. The fans were straightforward components to model since in normal operation, they have three set speeds that operate at a specific wattage. The power consumed by the fan was known from the product data and a multimeter, but to determine the volumetric flow rate of the fan at the different speeds, airflow testing had to be completed. The FF fan modeled in AMESIM is shown in Figure 3-8.

model and the split was determined by airflow testing through the convertible drawer.



Figure 3-9 Airflow Test setup for convertible drawer flow measurement

3.3.4 Creation of Refrigerator/Freezer Cabinet and the Control Algorithm

A CREO model of the refrigerator-freezer test unit (shown in Figure 3-10) of the refrigerator was available to pull dimensions from. Information such as wall thickness, height and width of compartments were added to the model. Figure 3-11 shows the FF cabinet modeled in AMESIM. The functions shown in the figure are the heat resistance circuit as the heat from the ambient convects on the outer case wall, conducts through the insulation (and possibly VIP), and convects into

the compartment. There are mullions filled with insulation foam that separates the compartments and limits the amount of heat transferred to each other. The mullions are modeled by implementing a one-dimensional heat flow circuit. A heat generation node was added to the FF and FZ compartments of the model. These nodes are what will be supplemented into the model as the heat leak values from the heaters are determined from the forward heat leak experiment.

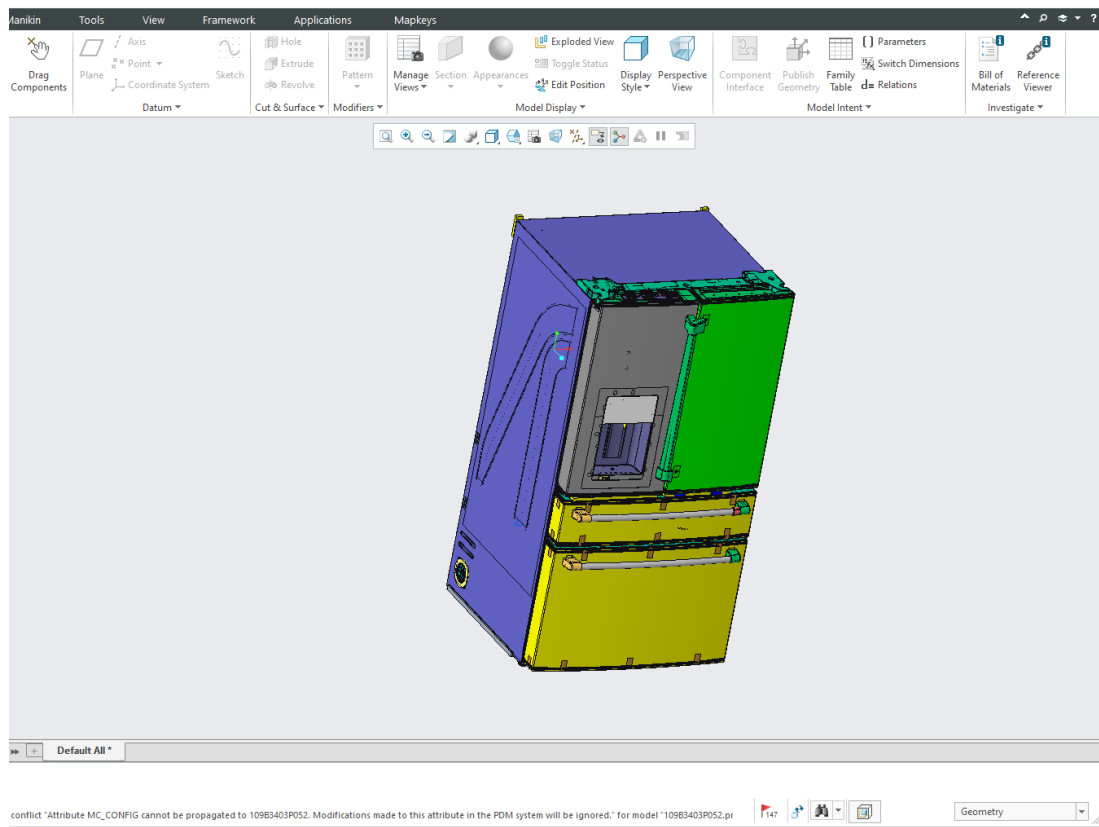


Figure 3-10 CREO Model of French Door Test Product

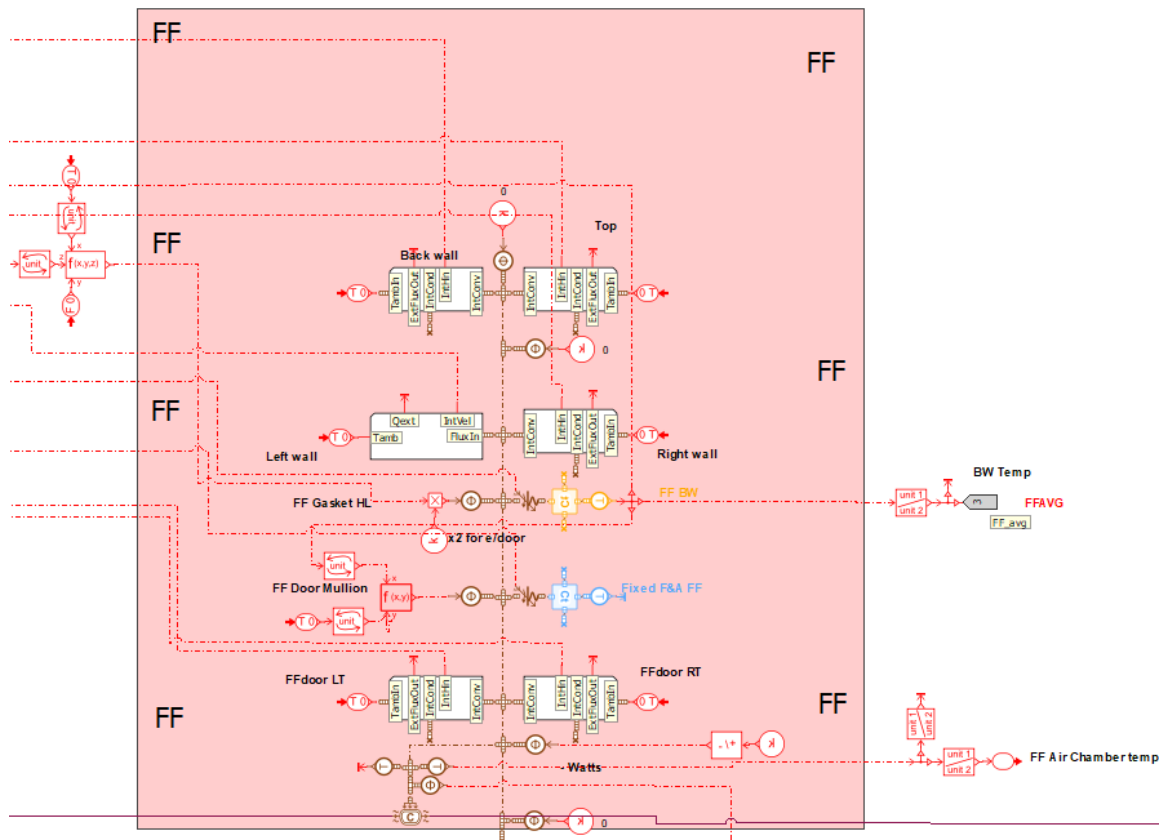


Figure 3-11 Fresh Food Cabinet supercomponent

The control algorithm for the AMESIM model mimics the control algorithm on the test unit. Due to intellectual property concerns, the control algorithm won't be discussed in full detail, however the unit operates by a two-dimensional grid control. Depending on the temperature in the fresh food and freezer, the compressor and fan speeds, as well as the damper position, will be at a specific value. Every combination of FF and FZ temperatures yields a different grid position and the use of "and" and "if" statements were used in the AMESIM model to replicate this logic. Replicating this was important as this logic determines how frequently the compressor needs to be on. The compressor only

turns off once all the cooling requirements of compartments are considered satisfied, and that condition is determined by the setpoints in the grid logic.

The results of the FWHL experiment will provide the rate of heat entering the compartment due to the operation of an anti-sweat component. The electrical heaters will be modeled by placing an additional heat leak offset in the appropriate compartments. The hot liquid loop was modeled differently as it is part of the hermetic system of the unit and therefore a part of the energy balance equation of the model. There is a benefit to the cooling capacity of the refrigerant when it goes through the liquid loop due to the fact that the refrigerant loses heat as it passes through the unit, therefore providing it with a colder starting point before it reaches the expansion device. There is a tradeoff associated with the use of the liquid loop due to the fact there is additional heat being introduced in the compartment along with additional cooling capacity given that the hot liquid loop acts as an additional condenser. The AMESIM model replicated this effect by including a node that simulated the total heat loss rate of the hot liquid loop which in turn decreased the refrigerant inlet temperature at the expansion device.

4 RESULTS

4.1 Heat Quantification Test Results

In order to estimate the total heat dissipated from the hot liquid loop, the test procedure described in 2.1 was performed. As mentioned prior, this test was performed on a refrigerator-freezer in normal cycle behavior, so the compressor control is oscillatory as it turns off whenever its compartment temperatures reach a satisfactory value and turns back on whenever the temperatures get too warm.

Figure 4.1 shows the heat load dissipated across the hot liquid loop over a period of time of steady refrigerator operation. The average heat load was taken over a period of 80 minutes (which reflects the on time for the compressor in a cooling cycle) when the unit was able to maintain an average temperature of 37°F in the fresh food, 29.5 °F in the convertible drawer and 0°F in the freezer \pm 1 degree (shown in Figure 4-2) and when there was not an abnormally high amount of pressure drop, such as when the compressor was on.

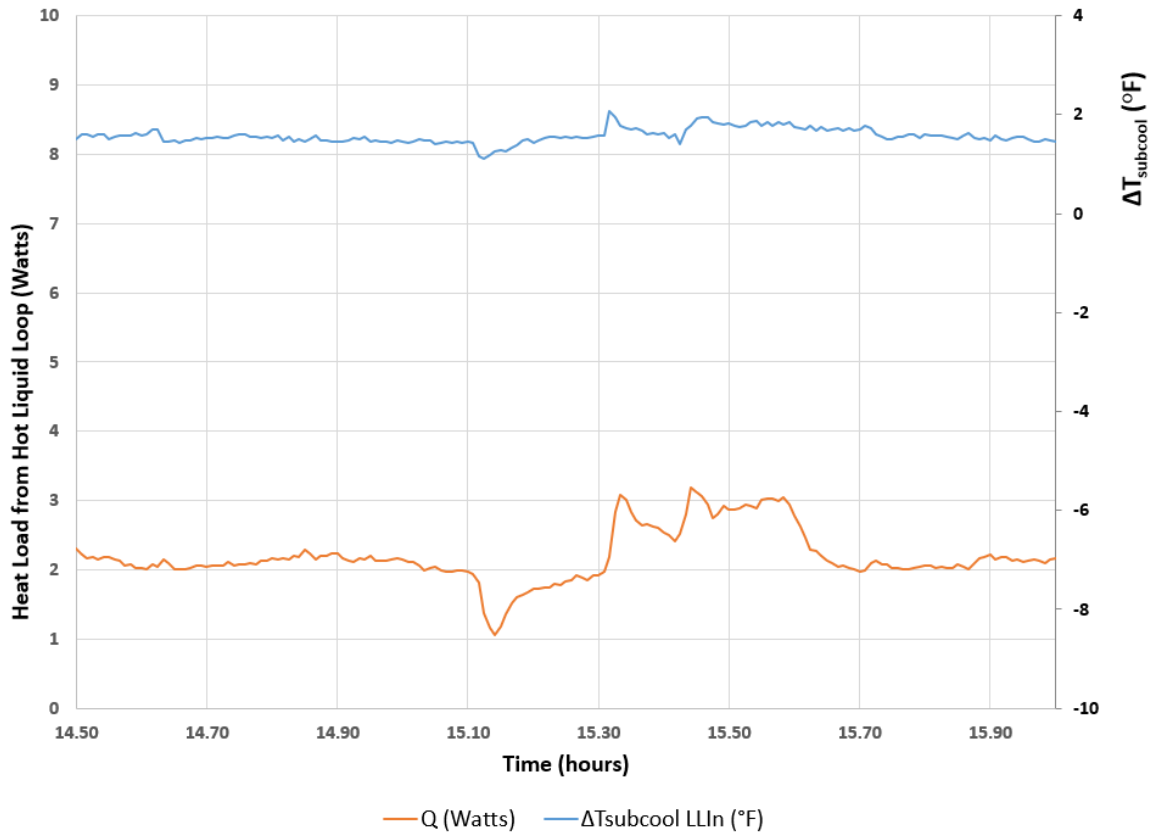


Figure 4-1 Heat load and subcooling at the inlet of hot liquid loop plotted over compressor on cycle

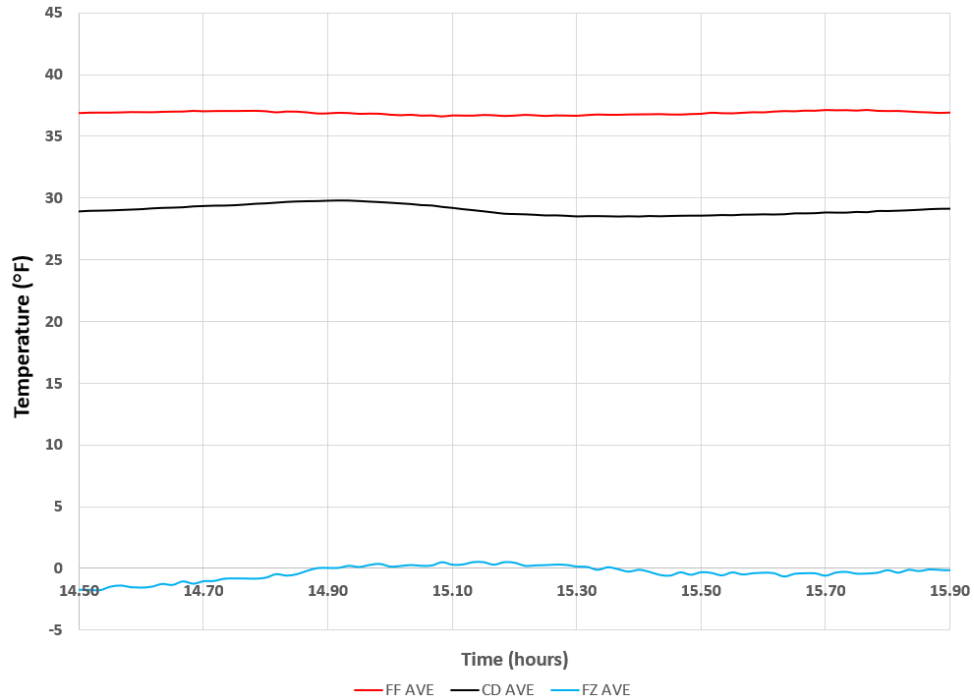


Figure 4-2 Compartment temperature stability in Heat Quantification Unit during compressor on cycle

Recall Equation 9 where the rate of heat loss by the hot liquid loop is equal to the mass flow rate times the change in enthalpy. The mass flow rate was calculated using Equation 10 and enthalpy at the inlet and outlet was defined by the pressure and temperature measurements taken at the inlet and outlet of the hot liquid loop. In order for the enthalpy measurements to be accurate based on just temperature and pressure, the refrigerant had to be single phase. To check whether the refrigerant at the inlet of the liquid loop was single phase, the level of subcooling of the refrigerant was calculated and plotted across the same period of time as heat load calculations. The degree of subcooling (shown in Equation 15) quantifies how far a fluid temperature is from the saturation temperature along the saturated liquid line and is equal to the

saturation temperature at a given pressure minus the actual temperature of the fluid. If the value is positive, that indicates the fluid is not two-phase, and is a subcooled liquid.

$$\Delta T_{subcoolLLIn} = T_{SatInlet} - T_{actual_{inlet}} \quad (15)$$

Averaging results from Figure 4-1 show that the total rate of heat dissipation (during a compressor on cycle) by the hot liquid loop is 2.4 W.

4.2 Forward Heat Leak Test Results

The test method described in section 2.2 was used to obtain the results presented in the following sections. By observing the difference in evaporator capacity of the FWHL system between the on and off states of these anti-sweat components, the total rate of heat entering the cabinet from each component was quantified. Data was taken after compartments and ambient reached ± 0.2 degrees of their targeted temperature over a span of at least 12 hours. That average was taken over a 12-hour period of stability and is the value reported throughout this study.

4.2.1 Electrical Anti-Sweat Heaters Test Data

The method for determining the fraction of heat coming from each of the heaters into the compartment was described in section 2.2. The heaters are foamed into the case of the refrigerator and not externally visible, however Figure 1-1 illustrates the location of each of the heaters. The noise present in the FWHL measurements is attributed to the system continually adjusting itself in order to maintain consistent temperatures. The data before any of the heaters are turned

on and without any hot water flowing through the system is shown in Figure 4-3 and Figure 4-4. This is the baseline data set and serves as the reference case to compare against the on states of each anti-sweat component. FF is the fresh food temperature and FF Q is the total heat leak in the FF compartment. FZ is the freezer temperature, CD is the temperature in the convertible drawer and FZ Q is the total heat leak in the FZ compartment.

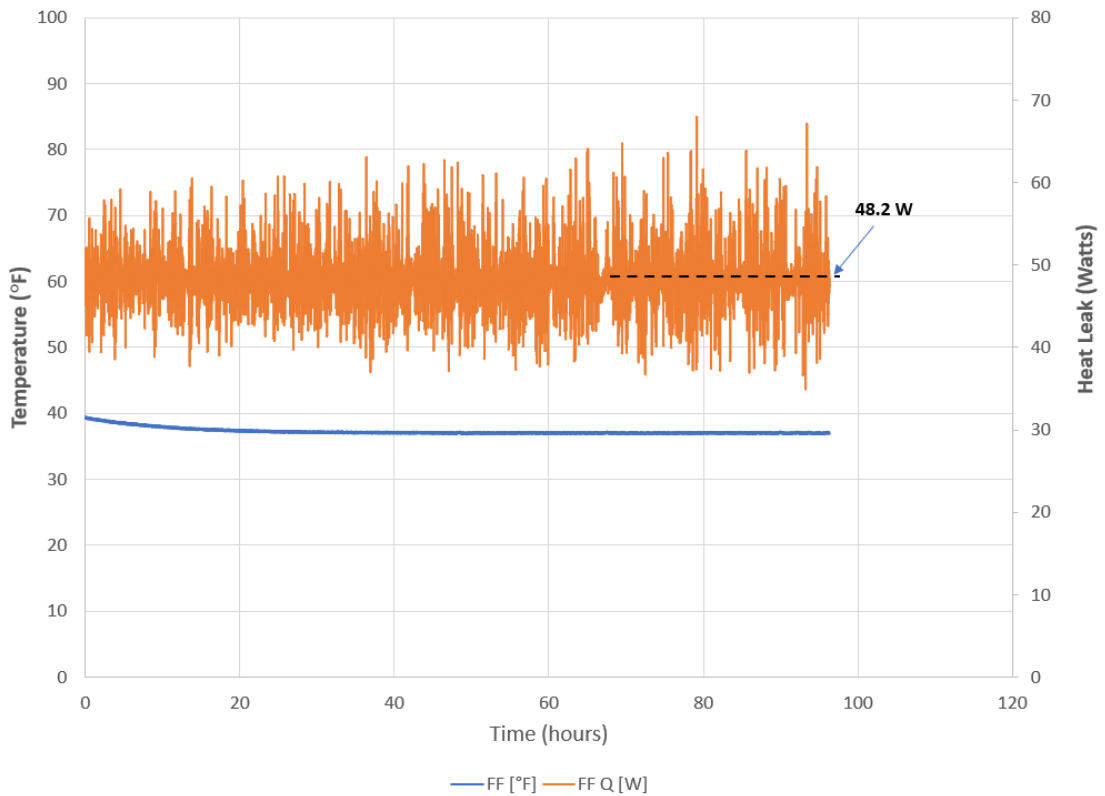


Figure 4-3 Baseline Heat Leak in the Fresh Food Compartment

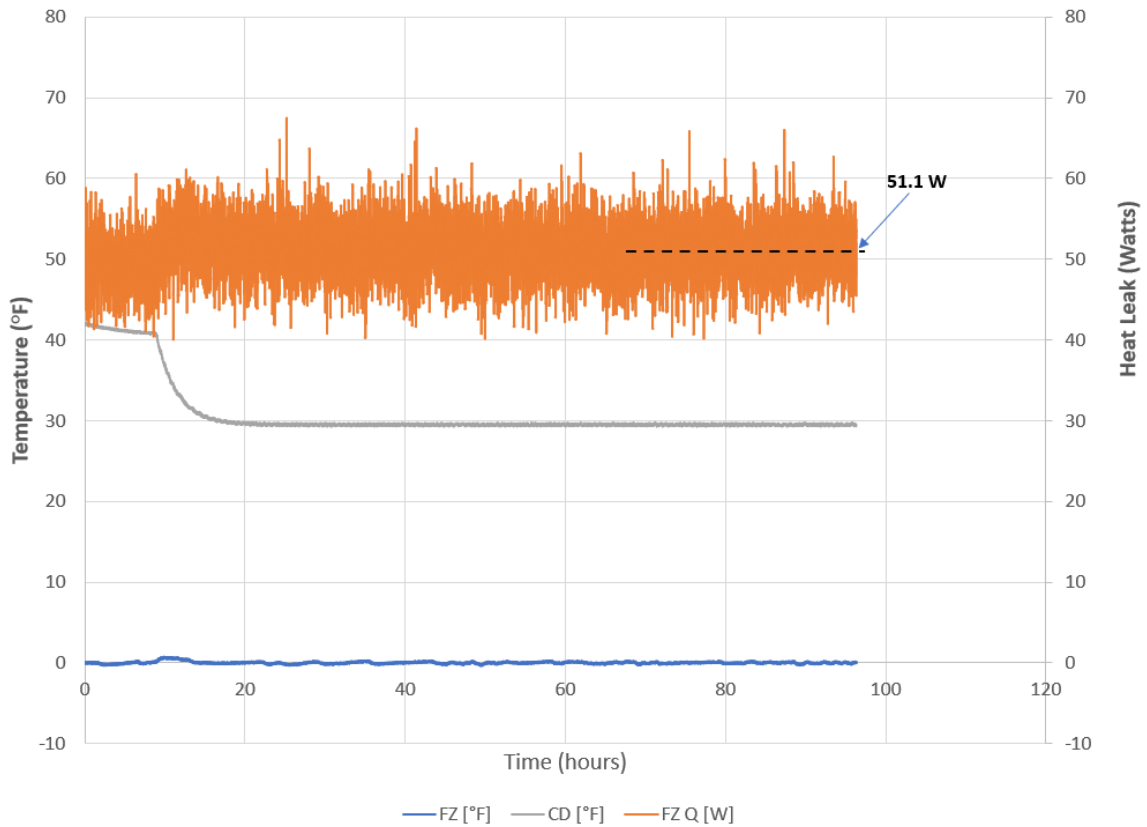


Figure 4-4 Baseline Heat Leak in the Freezer Compartment

The effect of the 10.9 W articulating mullion heater after it is turned on is shown in Figure 4-5 & Figure 4-6. The baseline heat leak in the FF is 48.2 W (shown in Figure 4-3) and once the articulating heater is turned on in it shows a heat leak value of 55.4 W (shown in Figure 4-5). The change in heat leak between the two values shows that there is 7.2 W entering into the FF compartment. The same calculation was repeated for the FZ compartment, which shows 0.6 W into the FZ. Given that the heater has a total heat load of 10.9 W and 7.8 W is calculated to go back into the compartment, it can be said that 71% of the heat from the articulating mullion heater enters back into the unit. This calculation process was repeated for all the anti-sweat components.

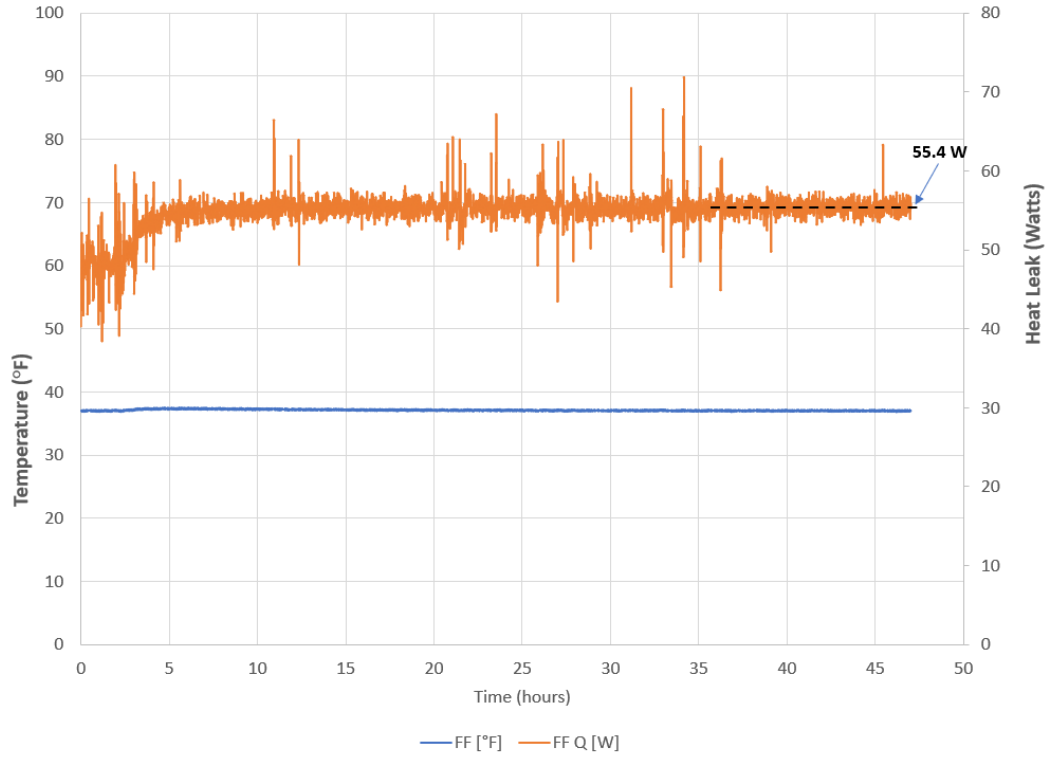


Figure 4-5 Heat Leak with Mullion Heater on in the FF Compartment

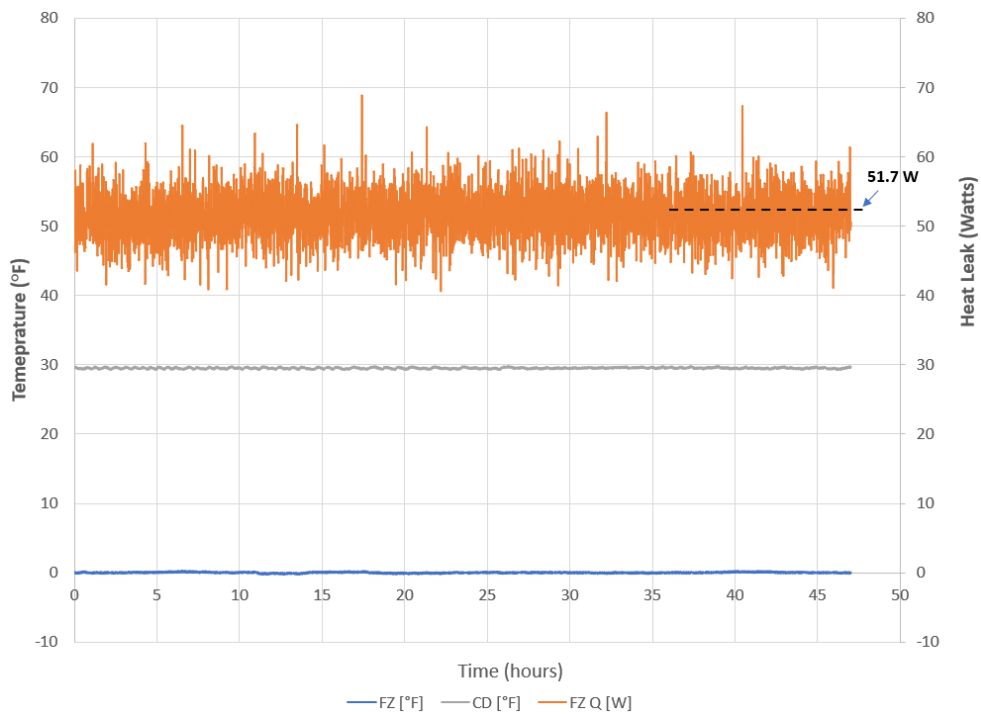


Figure 4-6 Heat Leak with Mullion Heater on in the FZ Compartment

The door in door heater output is 10.5 W and is located on the right door panel. Figure 4-7 provides an image of the door in door portion and where the heater is located. The data after the heater is turned on is shown in Figure 4-8, and it shows that there is 5.3 W entering back into the FF compartment and Figure 4-9 shows 0.2 W into the FZ compartment.



Figure 4-7 Anti-Sweat Heater inside Door in Door Liner

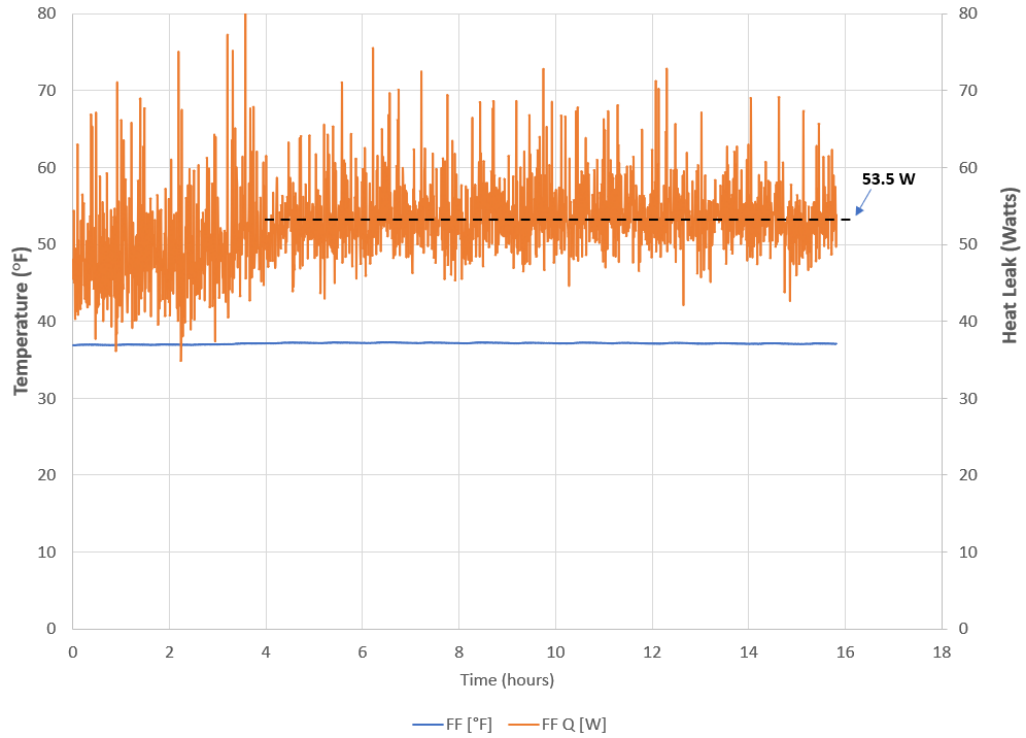


Figure 4-8 Heat Leak with Door-In-Door Heater on in the FF Compartment

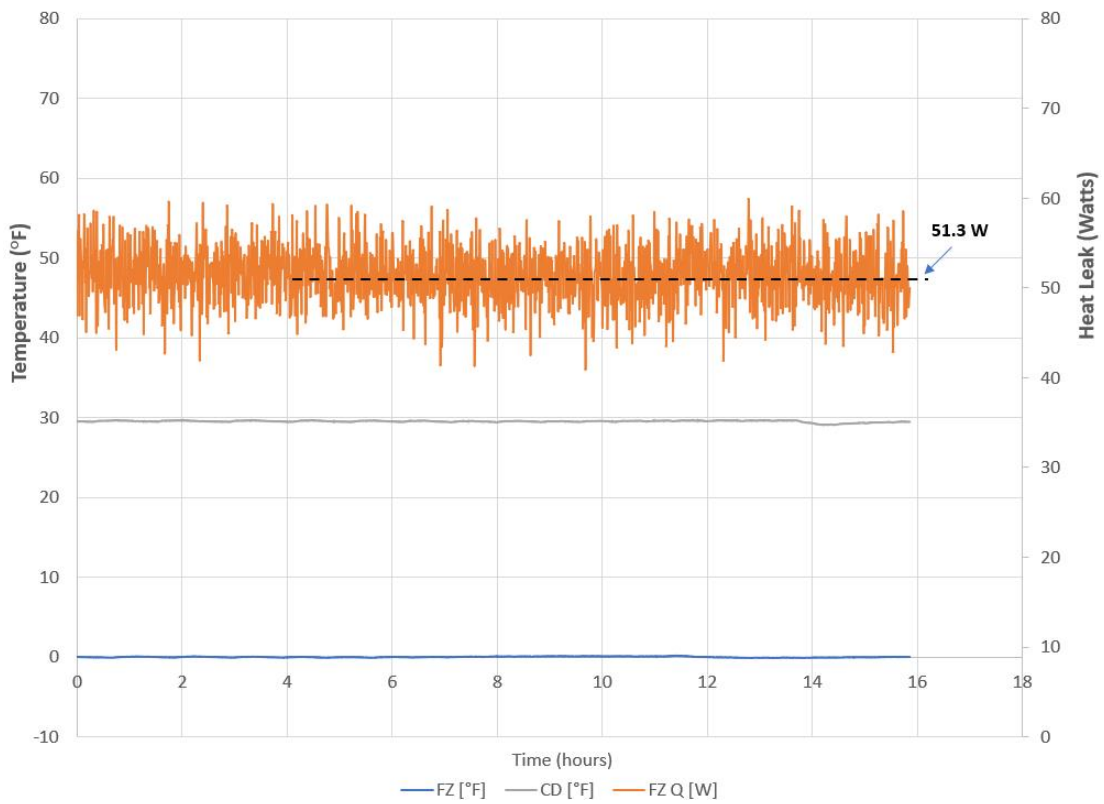


Figure 4-9 Heat Leak with Door-In-Door Heater on in the FZ Compartment

The icebox gasket heater is located in the icebox area. The total output of this heater is 5 W. Figure 4-10 shows the heat leak in the on condition and shows that the change in heat leak entering the FF compartment between the baseline is 1.6 W and Figure 4-11 illustrates the impact to the FZ is negligible.

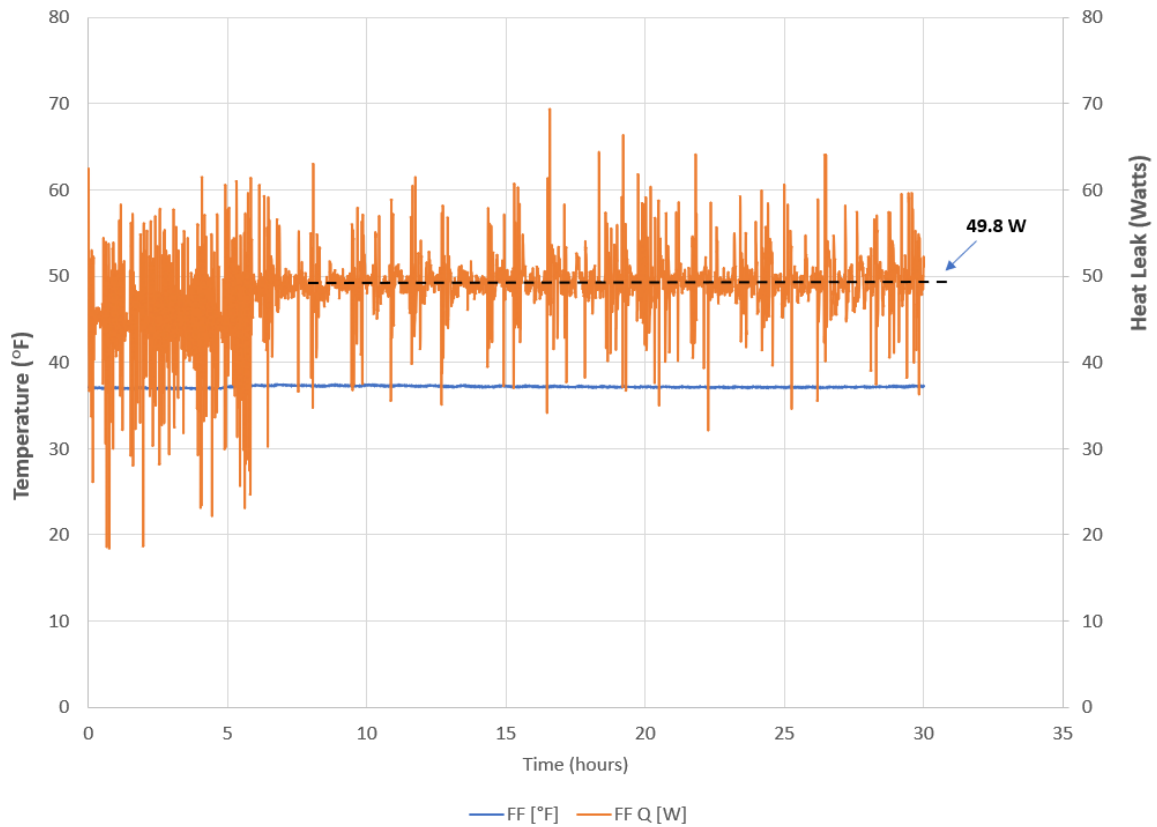


Figure 4-10 Heat Leak with Icebox Gasket Heater on in the FF Compartment

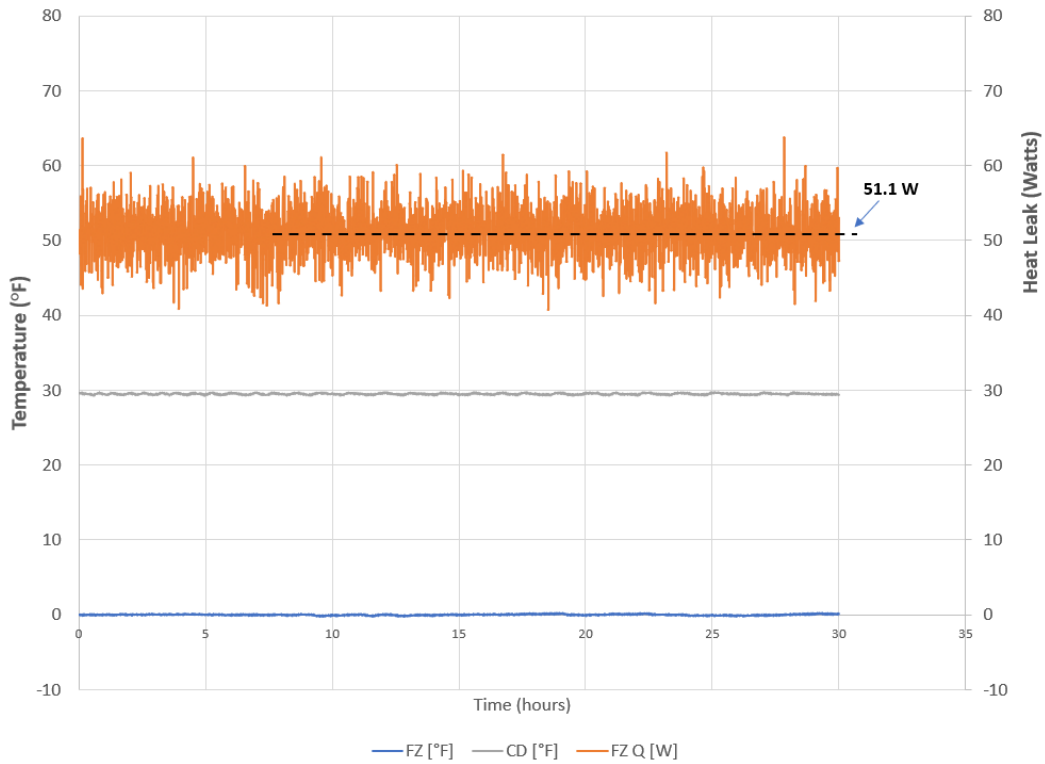


Figure 4-11 Heat Leak with Icebox Gasket Heater on in the FZ Compartment

The ice dispenser heater is located in the water/ice dispenser area and is a 1.25 W heater. Figure 4-12 and Figure 4-13 show the heat leak measured when the heater is turned on, and there is no noticeable change in heat leak from the baseline.

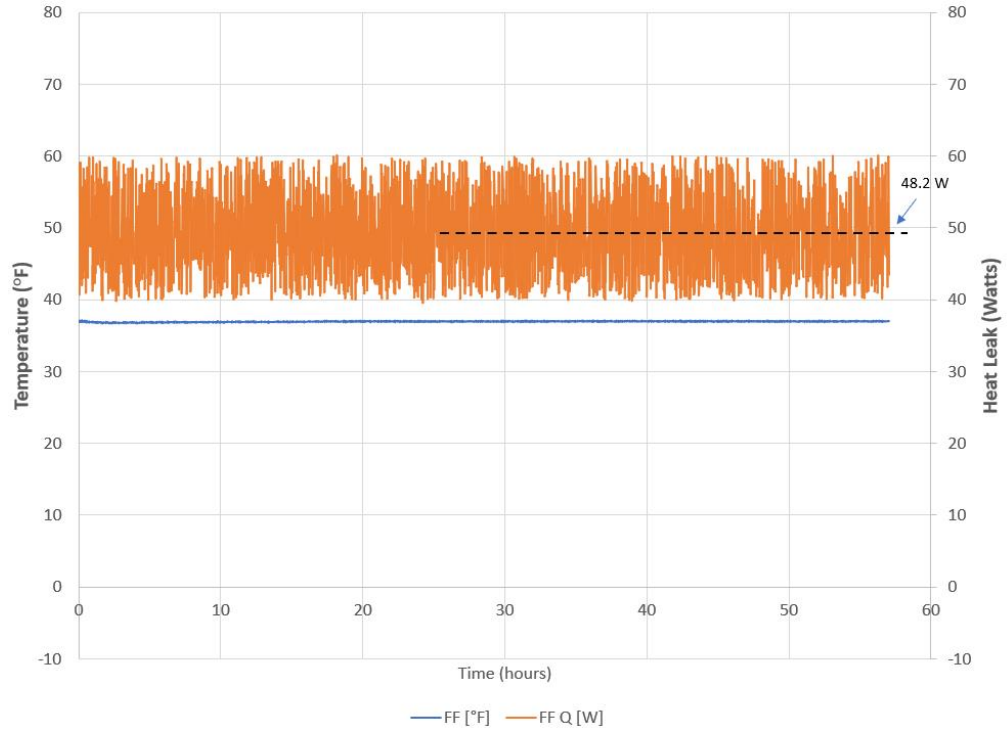


Figure 4-12 Heat Leak with Ice Dispenser Heater on in the FF Compartment

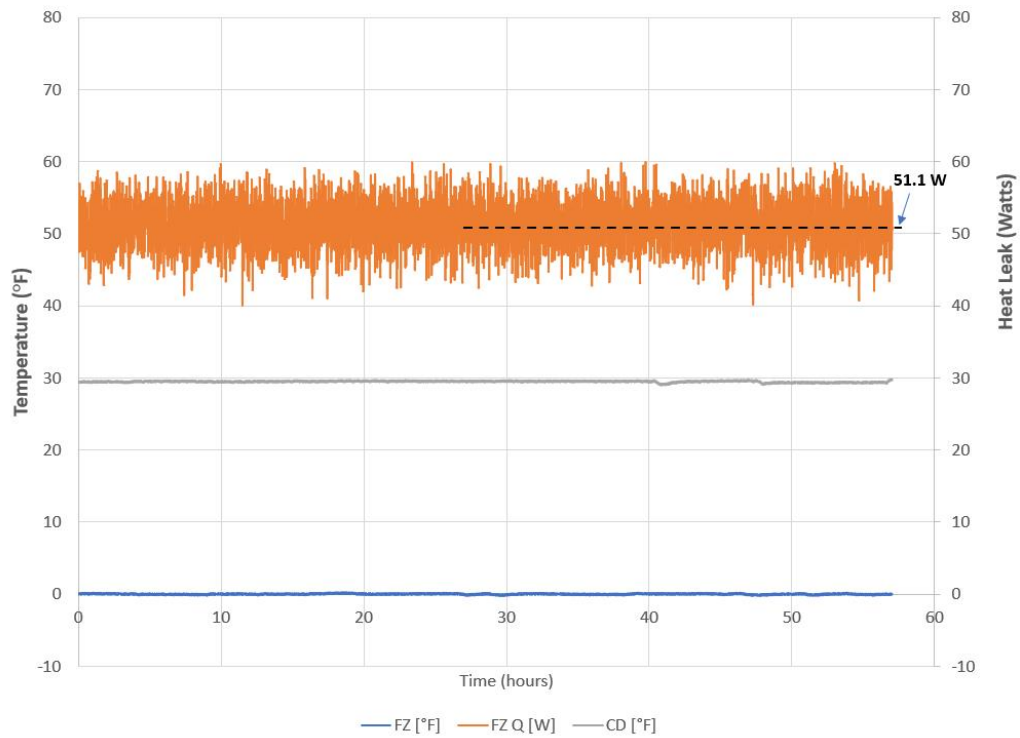


Figure 4-13 Heat Leak with Ice Dispenser Heater on in the FZ Compartment

4.2.2 Hot Liquid Loop Data

The procedure for modeling the heat load of the hot liquid loop was described in section 2.5. The total amount of heat being dissipated by this hot liquid loop was found to be 2.4 W. Given the large size of the pump installed in the hot water system, it was not feasible to control the water flow to such low levels accurately recreate a 2.4 W heat load. Recall that the heat load of the water is directly proportional to the mass flow rate of the water and the inlet and outlet temperatures. With the expected temperature difference being about 1°F, the mass flow rate of the water would have to be controlled to 1-2 lbm/hour which was not possible with the equipment used in this experiment.

A revised plan to determine the fraction of heat entering the cabinet was to model the hot liquid loop using a larger heat load. Given the pump was not capable of flows below 100 lbm/hr, the inlet temperature of the water was matched to that of the refrigerant seen in the heat quantification study so that the difference in temperature between the working fluid (hot water in the case of the FWHL and R600A in the actual unit) and the compartment remained close to one another. With the metric in place, the inlet temperature of the water was set to 100 °F and the mass flow rate was set to 118 lbm/hr which provided a similar outlet temperature as the heat quantification unit. This equaled to a 30.5 W heat load and was modeled instead so that the hot water system could maintain a consistent heat load. The ratio of heat entering into the compartment from the hot liquid loop compared to its total heat load was assumed to be equal with varying heat load values.

The data taken with the hot water circulating through the system to model the hot liquid loop is shown in Figure 4-14 and Figure 4-15. The total heat load of the hot liquid loop in this Forward Heat Leak experiment was shown to be 30.5 W and the data shows that about 21.7 W go into the freezer and 0.8 W into the fresh food. This equates to a total of 22.5 W or 74% of the total heat load goes back into the freezer and convertible drawer compartment. If we assume linear proportionality, that equates to **1.8 W** of the **2.4 W** hot liquid loop goes back into the freezer and convertible drawer compartment in normal on operation.

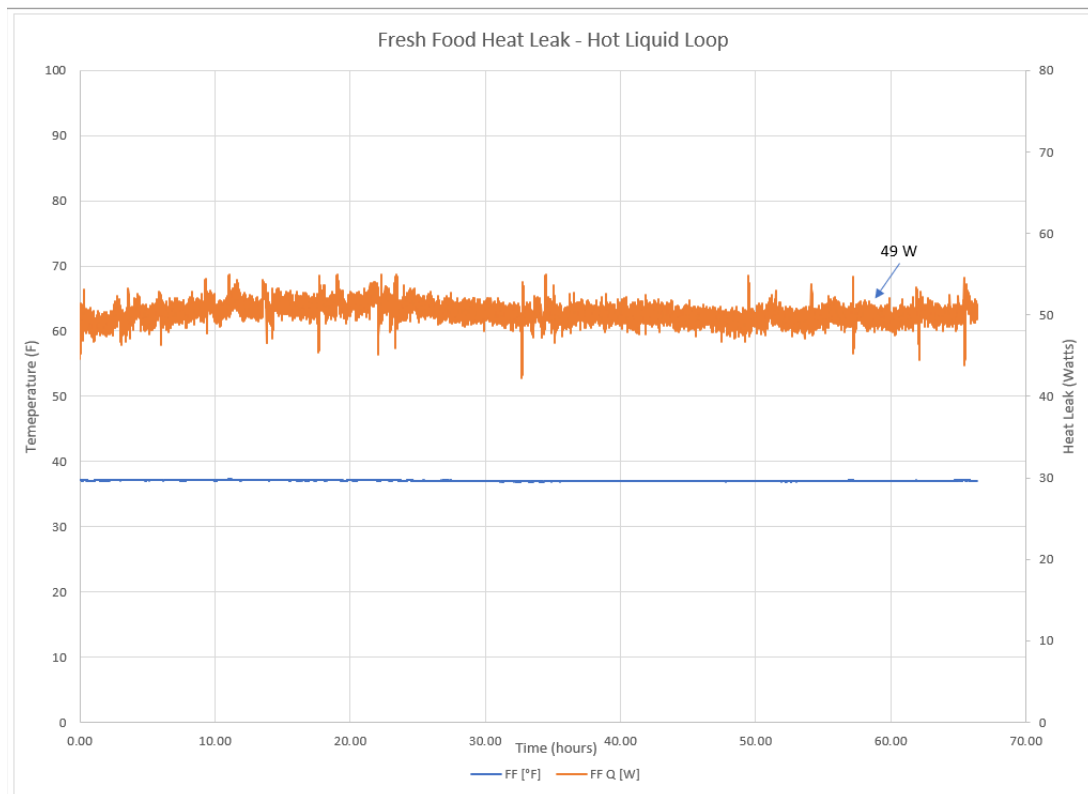


Figure 4-14 Heat Leak with Hot Liquid Loop on in the Fresh Food Compartment

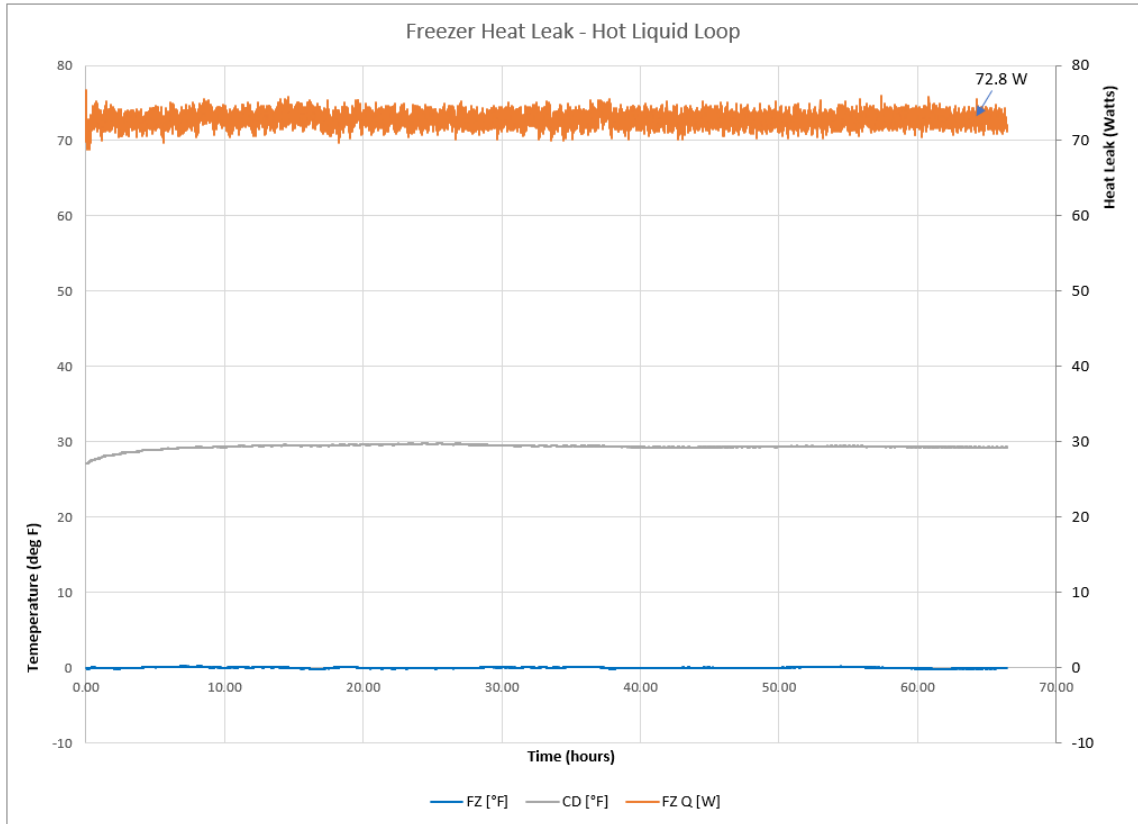


Figure 4-15 Heat Leak into the FZ Compartment with Hot Liquid Loop Activated

4.2.3 Summary of Forward Heat Leak Test Results

Table 4-1 provides a summary of all the results from the forward heat leak experiment. The 1.8 W value in the hot liquid loop row is calculated from applying the same ratio of heat entering the compartment from the hot water loop to the total heat load of the hot liquid loop, so $2.4 \text{ W} * 74\% = 1.8 \text{ W}$. Based on the data, it appears that the articulating mullion sent the most heat into the compartment, followed by the door in door heater, and icebox gasket heater. The ice dispenser heater provided negligible heat load to the cabinet.

The fraction of heat entering back into the compartments from the heaters located in the icemaking area appear to be much less than the other anti-sweat

components. The total heat loads of the ice area heaters were lower which could have played a role since temperature difference drives heat transfer. The ice making area is also highly insulated in comparison to other areas of the refrigerator in order to keep the temperature cold enough for ice formation. In comparison to the other anti-sweat components, the heat generated from the ice area heaters have a more heat resistive network to pass through than the others before reaching the compartment and likely dissipated much of the heat into the surroundings.

Name of Heat Source (Anti-Sweat Component)	Total Heat Load (Watts)	Heat Entering the Compartment (Watts)	Percent of Heat Entering the Compartment
Hot Water Loop	*30.5	22.5	74%
Hot Liquid Loop	2.4	1.8	74%
Articulating Mullion Heater	10.9	7.8	71%
Door-In-Door Heater	10.5	5.5	52%
Icebox Gasket Heater	5	1.6	32%
Ice Dispenser Heater	1.25	Negligible	0%

Table 4-1 Summary of Forward Heat Leak Test Results for each Anti-Sweat Component; *Scaled up heat load to model hot liquid loop in FWHL.

4.2.4 Repeatability Testing for Forward Heat Leak Experiment

The forward heat leak experiment with the electrical heaters was repeated to check repeatability of results. A new baseline was obtained, and the test procedure was repeated for the four heaters. A summary of the results with a percent different between the original results are shown in Table 4-2. Largest

error between the two test runs was at 8%, providing more confidence in the results presented in the Forward Heat Leak study.

	Heat Entering the Compartment; 1 st Run (Watts)	Heat Entering the Compartment; 2 nd Run (Watts)	Error Between the Two Runs
Articulating Mullion Heater	7.8	8.2	4.8%
Door-In-Door Heater	5.5	5.05	8.2%
Icebox Gasket Heater	1.6	1.5	7%
Ice Dispenser Heater	Negligible	Negligible	0%

Table 4-2 Repeated test results of the Forward Heat Leak Experiment

4.3 AMESIM Model Test Results

The AMESIM model was used in order to look at the energy impact and thermal performance of the unit based on the heat leak going into the compartments from the anti-sweat components. In order to correlate the model, brass weights were used to capture average compartment temperatures and thermocouples that measure the outlet air temperature of the evaporators provide correlation for the model to improve upon the parameters such as the wall heat transfer coefficients to ensure accurate prediction of the model. The AMESIM baseline model was validated by comparing the run time as well as cycle behavior to a refrigerator-freezer in normal operation and the results of the comparison are shown in Figure 4-16. The test unit had a compressor run time of 84.3% and the AMESIM model showed an 85.3% runtime. Similarities in

compressor and cycle behavior provided confidence in AMESIM model as a predictive tool for heat leak study.

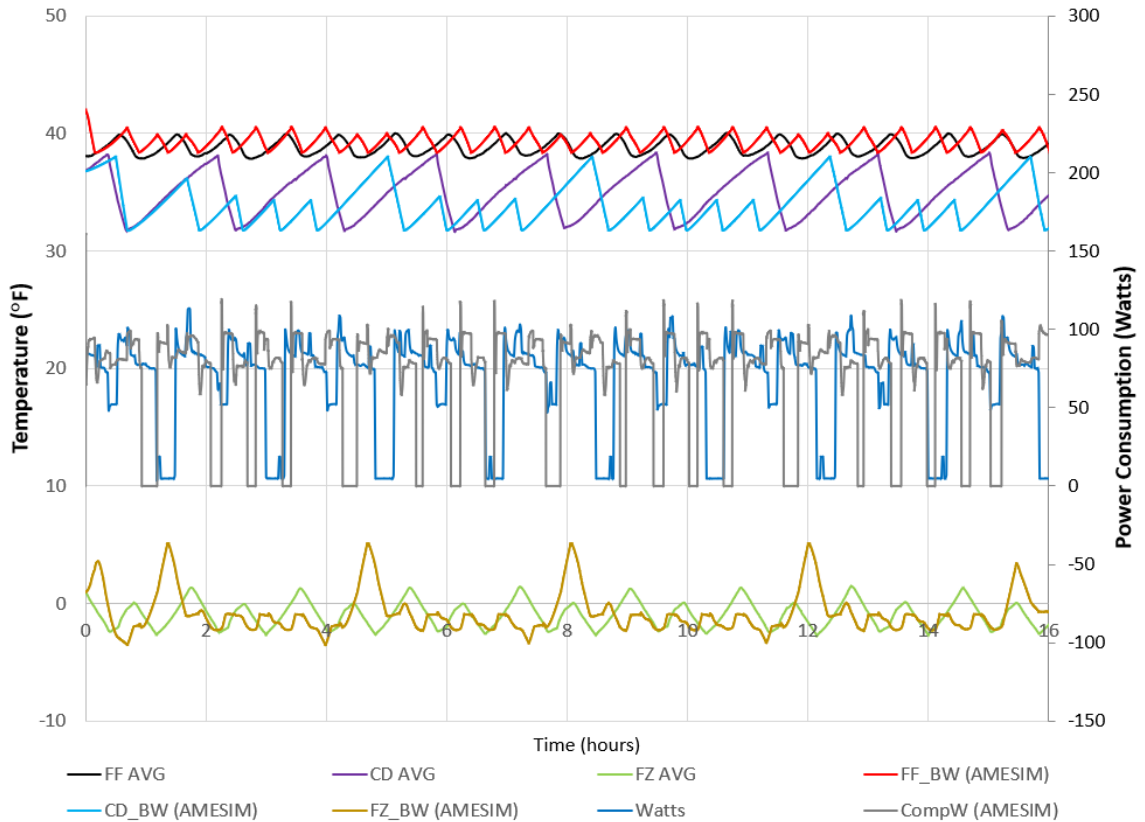


Figure 4-16 Comparison between AMESIM model and test data from a real unit

With the heat load into the compartment quantified for each of the anti-sweat components (values shown in Table 4-1) an AMESIM study was conducted in order to see how much that additional heat leak amount impacts compressor power consumption and thermal performance. Although the heaters do not run 100% of the time in actual operation, they were tested in the FWHL experiment as such to effectively understand how much the operation of the heaters affect compressor power consumption and the general thermal performance in terms of keeping the compartment at the desired setpoint. There

were heat generation nodes in the FF and FZ compartments in the AMESIM model for each of the heater's heat leak contribution and the results are shown below in Table 4-3.

	FF	CD	FZ	Compressor	Compressor
	[°F]	[°F]	[°F]	RT%	Power [W]
Baseline	38.2	31.5	0.8	85.3	84.9
Articulating Mullion Heater [7.8W]	38.2	31.9	1.2	90	86.7
Door-In-Door Heater [5.5W]	38.3	31.2	0.6	84.2	86.8
Icebox Gasket Heater [1.6W]	38.3	31.1	0.5	82	85.8
Hot Liquid Loop [1.8W]	38.4	30.1	-0.5	75.7	87.8

Table 4-3 AMESim Model Results given additional heat leak inputs from anti-sweat components

With the articulating mullion, the additional heat leak from the heater creates an additional 1.8 W for the compressor power, (found by subtracting the heater-on compressor power from the baseline which is 86.7 W - 84.9 W) 4.7% increase in run time while slightly warmer in FZ and CD. The Door-In-Door heater caused a decrease in run time by 1% but increased compressor power consumption by 1.9 W. The heat from the icebox gasket heater decreased compressor runtime by 2% but increased compressor power by 1 W. The hot

liquid loop is part of the hermetic system, and its operation is based on the state of the compressor. The compressor run time decreased by about 10% however power consumption increased by 2.9 W while temperatures in the FZ and CD were colder.

4.4 Uncertainty Calculations with Test Results

For all the instrumentation used throughout, there was an uncertainty associated with each of the readings from the RTDs and pressure sensors which accumulated into a total absolute uncertainty. The two primary outputs of data calculated in this study were the heat load from the hot liquid loop (Eqn. 9) and evaporator cooling capacity (Eqn.13) which was described as the heat leak.

The sequential perturbation method was used to estimate the uncertainty for the measurements which uses the finite difference of each of the variables to approximate the derivatives and calculate a total absolute uncertainty of the measurement. The absolute uncertainty is provided by the manufacturers of the sensors. The RTDs measurements had an uncertainty of 0.25% based on the measurement reading, mass flow meter was 0.1% of reading, and the pressure transducers were 0.05% of reading. The uncertainty results are shown in Table 4-4 and 4-5.

	Mean	Absolute	Relative	Individual Contribution
	Value	Uncertainty	Uncertainty	to Uncertainty
c_p [Btu/lbm°F]	1.00	0.0	0.0	0
\dot{m} [lbm/h]	118.11	0.118	0.1%	0
T_{in} [°F]	100.00	0.250	0.3%	50.5%
T_{out} [°F]	99.00	0.248	0.3%	49.5%
\dot{q} [Btu/h]	118.11	41.550	35.18%	N/A

Table 4-4 Uncertainty Calculation for the heat leak results in Hot Water System
Liquid Loop

The relative uncertainty of the hot water system liquid loop was calculated at 35.18%, with averages taken from the stable period of the experiment. As shown in Table 4-4, the uncertainty from the mass flow meter was negligible and all the uncertainty was driven by the RTD temperature measurements. Since the difference in temperature between the two RTDs was extremely low at 1.0°F, the margin of error for the measurements was low as well hence the higher relative uncertainty. At a temperature difference of 2.0°F, the relative uncertainty drops to 17.5% and at 4.0°F it drops down to 8.66%. The absolute uncertainty of the RTD is at 0.25 °F at 100°F, and it shows that a change of T_{in} of 0.25°F (which is the absolute uncertainty of the RTD) can impact $Q_{HeatLeak}$ by $29 \frac{Btu}{h}$ or 8.5 W. This high level of uncertainty is an area that needs to be addressed in future work.

	Mean	Absolute	Relative	Individual Contribution
	Value	Uncertainty	Uncertainty	to Uncertainty
\dot{m} [lbm/h]	3.7	0.004	0.1%	1.2%
h_{in} [Btu/lbm]	102.5	0.308	0.3%	26.9%
h_{out} [Btu/lbm]	167.5	0.503	0.3%	71.9%
\dot{q} [Btu/h]	239.2	2.181	0.91%	N/A

Table 4-5 Uncertainty Calculation of the heat leak results for the Forward Heat Leak System

The relative uncertainty of the forward heat leak calculation was very low at 0.91%. An absolute uncertainty was taken by observing the difference in enthalpy calculation based on the average value of the RTDs and pressure transducers. Since such a large temperature difference exists between the RTDs, the uncertainty is relatively low. A change of T_{in} and P_{in} of 1.1°F and 1 psia respectively can impact \dot{q}_{evap} by $1.47 \frac{\text{Btu}}{\text{h}}$ or 0.43 W.

5 CONCLUSIONS

5.1 Important Results

The goal of this study was to quantify how much heat from anti-sweat components in a household refrigerator-freezer is transferred into the fresh food and freezer compartments and how that additional heat leak impacts compressor power and thermal performance. A forward heat leak calorimeter system was used to quantify the amount of heat entering the compartments and an AMESIM simulation model was used to run a model that predicted the compressor power consumption with the additional heat leak values. The key results from this study are summarized in the following bullets.

- From the 30 W that is generated from the anti-sweat components, a total of 16.7 W was calculated as the amount of heat that enters back into the cabinet with a relative uncertainty of less than a percent.
- The largest contributor for heat leak into the cabinet is the articulating mullion heater, with a total of 10.9 W generated by the heater and, based on the forward heat leak experiment 7.8 W entered into the cabinet. Using the AMESIM model, the operation of

- this heater will increase power consumption of the compressor by 1.8 W and run time by 5%.
- The 2nd largest contributor was the Door-In-Door heater. 10.5 Watts is emitted from the heater and the FWHL experiment shows that 5.5 W entered into the compartment. The AMESIM predicts an additional 1.9 W of compressor power consumption to overcome this heat load.
- The icebox gasket heater emitted 5 W and the FWHL experiment shows that about 1.6 W entered into the compartment. The AMESIM predicts an additional 0.8 W of compressor power consumption.
- Tests showed the hot liquid loop dissipated a total of 2.4 W of heat. Due to instrumentation constraints, the forward heat leak system could not accurately measure such a small heat rate and a test was run at a much rate and this data predicted 74% of the heat entered into the cabinet. This equates to 1.8 W of the total 2.4 W for the hot liquid loop. Based on results from AMESIM, the compressor consumption increased by 3.0 W although run time went down 10%.
- The smallest contributor to heat leak was the ice dispenser recess heater which was dissipated 1.25 W total. Based on the forward heat leak experiment, this had negligible impact.

- The measurement technique for the heat leak in the FWHL was accurate and within a percent of error and the hot water system required a higher temperature difference to obtain a low uncertainty in test results as relative uncertainty was at 35% for that system.
- Forward heat leak tests were rerun for all the electrical heaters with a different baseline. All results were within an 8% difference providing more confidence in the accuracy of the results.
- Overall, the rate of heat introduced into the cabinet from operating the anti-sweat components continuously for a year account for about 66.5 kWh/year which would be 9.5% of the total annual usage of the product
- Given refrigerator appliances are generally designed to address the worst case sweat conditions, optimal implementation of the anti-sweat components is critical in ensuring DOE energy standards will be met for years to come

5.2 Future Work & Conclusion

Testing the anti-sweat heaters under the conditions specified in the AMESIM model for an extended period of time on an actual unit would be a way to validate the results provided by AMESIM. Heaters would have to be powered independently to ensure they run 100% of the time. A minimum of three units for testing is recommended to account for unit-to-unit variance.

An area of improvement for this experiment is the hot water system (used as a surrogate for the hot liquid refrigerant loop) as the uncertainty of the calculations was high relative to the heat load calculations. Equipment was a limiting factor in this experiment but one way to improve it would be higher accuracy RTDs as the temperature difference of 1.0°F seen in this experiment proved to be too small for the sensors to accurately measure the heat load. There was also an issue of the pump circulating the water being oversized for this application. A much smaller pump and high accuracy mass flow meter capable of reading 1 lbm/hr would be necessary for an accurate hot water system.

Another alternative would be to have a R600A refrigerant-based system as opposed to the water to model the hot liquid loop in the FWHL system. Even though water and R600A have different specific heat capacities, the assumption for this study was that due to the low temperature gradient the hot liquid loop sees in normal operation, water would be able model the hot liquid loop accurately enough. The validity of this claim was not explored in this study and can be looked at in the future.

Another assumption made in this study was that the hot liquid loop is that the fraction of heat leak to total heat load for the hot liquid loop is a constant, irrespective of the total heat load. Additional test runs at higher mass flows could have tested the validity of this claim, but time was the limiting factor and was not explored in this study.

The forward heat leak calorimeter system proved to be an effective way of determining heat gain into a cabinet from the anti-sweat components and the components provided a non-negligible impact on compressor power required or compressor run time. The AMESIM model also proved to be a useful tool in simulating the refrigerator-model performance used in this study and provided insight on refrigerator performance as a result of the additional heat leaks. From the results of the experiment, there was an established confidence in the ability of accurately measuring heat gain in the compartments as well as having a much better understanding of how much energy is actually expended on these refrigerator-freezer units to combat the issue of sweat.

REFERENCES

- Appliances, M., Refrigerators, F., Refrigerators, F. and Refrigerator, C., 2022. *Café™ ENERGY STAR® 27.8 Cu. Ft. Smart 4-Door French-Door Refrigerator/CVE28DP2NS1*. [online] Cafe Appliances. Available at: <<https://www.cafeappliances.com/appliance/Cafe-ENERGY-STAR-27-8-Cu-Ft-Smart-4-Door-French-Door-Refrigerator-CVE28DP2NS1>> [Accessed 7 May 2022].
- Alqaity, A. B. S., Al-Dini, S. A., & Zubair, S. M. (2013). Effectiveness-NTU relations for parallel flow heat exchangers: The effect of kinetic energy variation and heat leak from outside. *International Journal of Refrigeration*, 36(5), 1557–1569.
- Berghuis, C. (2020). Experimental evaluation of heat leak and convective heat transfer in a household freezer.
- Chen, L., Sun, F., Wu, C., & Kiang, R. L. (1997). A generalized model of a real refrigerator and its performance. *Applied Thermal Engineering*, 17(4), 401–412.
- Chen, L., Wu, C., Sun, F. (1998). Influence of internal heat leak on the performance of refrigerators. *Energy Conversion and Management*, 39(1-2), 45–50.
- Dalkilic, A. S., & Wongwises, S. (2011). Experimental study on the modeling of condensation heat transfer coefficients in high mass flux region of refrigerant hfc-134a inside the vertical smooth tube in annular flow regime. *Heat Transfer Engineering*, 32(1), 33–44.
- Dorfman, A., & Fridman, E. (2006). Vapor quality measurement by a discharging calorimeter. *Fluid Phase Equilibria*, 244(1), 46–51.

Herrera, C. (2018). Internal GEA AMESIM study on the effect of condenser airflow on Integrated single evaporator product

Herrera, C. (2019). Internal GEA AMESIM study predicting performance of a top mount refrigerator

Li, J., & Hrnjak, P. (2017). Improvement of condenser performance by phase separation confirmed experimentally and by modeling. *International Journal of Refrigeration*, 78, 60–69.

Sahoo, R. K. (1989). Exergy maximization in refrigeration storage units with Heat leak. *Cryogenics*, 29(1), 59–64.

Sevilgen, G., Bayram, H., & Kilic, M. (2020). 1D analysis of cool down simulation of vehicle HVAC system. *Thermal Science*, (00), 99–99.

Wang, S., Gu, J., Dickson, T., Dexter, J., & McGregor, I. (2005). Vapor Quality and performance of an Automotive Air Conditioning System. *Experimental Thermal and Fluid Science*, 30(1), 59–66.

CURRICULUM VITA

NAME: Delva Felissaint

CONTACT INFORMATION: 6800 Steeprun Road, KY 40241
Work: 502-452-7460
Cell: 305-801-9878
delvafeli@gmail.com

DOB: July 3rd, 1996

EDUCATION & TRAINING M.S. Mechanical Engineering (exp. 08/2022)
University of Louisville
2019-2022

B.S. Mechanical Engineering
Florida International University
2014-2018

WORK/INTERNSHIP EXPERIENCE

General Electric Edison Engineer **August**
2019-August 2022

- Extensive work in thermal system team that included airflow testing, algorithm development, hermetic component design and other relevant work
- Research project on heat quantification from sealed system components which involved creating thermals simulation study as well as extensive DAQ system instrumentation
- Designed an oven cooling system and proved out feasibility with airflow studies

- Performed tolerance and stress study on F&A parts that led to redesign of components
- Created dryer prototype unit and showed feasibility on new airflow manifold design

CERTIFICATIONS

- E.I.T License and Certification
- GD&T Technologist Certification
- Creo and SolidWorks Fundamentals Certification

SKILLS & LANGAUGES

- Fully fluent in English and Haitian Creole
- Microsoft Office, Creo/ProE, Solidworks, Statistical Analysis, Airflow Testing, Calorimetry, DAQ Instrumentation, Excel Macros, C++ Prog, RefProp, EES, Mintab, Coil Desginer, AMESIM, Labview, MATLAB